Chapter 3

DIRECTED ASSEMBLY OF POLYOXOMETALATES ACROSS LENGTH SCALES: FROM MACRO-MOLECULES TO MICROSYSTEMS AND ICHELLS

ANTOINE G. BOULAY, GEOFFREY J. T. COOPER
and LEROY CRONIN*
School of Chemistry, WestCHEM
The University of Glasgow, University Avenue
Glasgow, G12 8QQ, UK.
**www.croninlab.com*

1. Building Blocks to Cation Control

Polyoxometalates (POMs) are discrete, anionic metal-oxide clusters of early transition metals. Composed principally of Mo, W, V and Nb, they represent a large and important class of inorganic molecules and materials,[1] whose relevance is being highlighted in a number of review articles, with an extraordinary reach in terms of applications, physical and chemical properties.[2,3] One of the most interesting aspects of POM chemistry is the underlying deceptively simple synthetic procedures.[4] Indeed, the overwhelming majority of the POMs isolated and reported to date in the literature are formed using straightforward "one pot" and one step conditions. Frequently, in this "one-pot" process, acidification of the precursor metal salts in aqueous solutions in the presence of chosen ingredients such as reducing agents, hetero-elements, counterions etc. leads to the formation of a variety of combinatorially linkable polyoxometalate building blocks in solution.[5] These small building blocks, formed by the edge- and corner-sharing of {MOx} units (where M = Mo, W; $x = 4 - 7$),

then self-assemble through condensation processes to form various cluster anions depending on the reaction conditions. In fact, these "one-pot" reactions can hide very complex solution speciation processes arising from the presence of a highly dynamical situation, that depends on a multitude of factors such as pH, ionic strength, reaction time, temperature, counterions, concentration of starting materials, presence of electron donors and their redox potential. However, recently, in our work we have shown how cation exchange reactions can be used not only to control assembly of the building blocks for POMs, but also direct their assembly into clusters, clusters-of-clusters, colloids, micro-structures and cellular compartments (see Fig. 1).

What makes understanding, not to mention control of the synthesis of POM clusters so difficult, is the sensitive dependence of the cluster architectures assembled with the reaction *and* crystallization conditions (see Fig. 2). This means that a barely detectable change in any given parameter

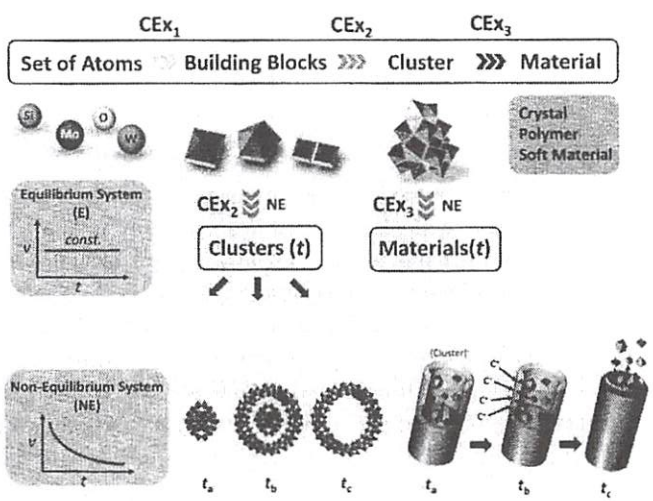

Fig. 1. Schematic representation of the top-down approach of POM synthesis under equilibrium and non-equilibrium conditions. The non-equilibrium approach allows the system to form time-dependant structures otherwise impossible to synthesize and/or characterize (t_a, t_b, t_c).

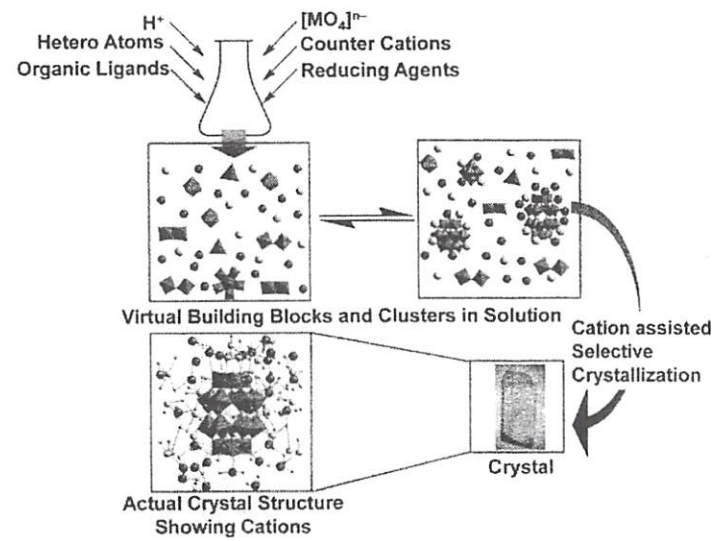

Fig. 2. Schematic representation of the traditional "one-pot" synthesis of POM clusters leading to the formation of various structural archetypes in solution highlighting the role of cations in selective crystallization of a particular product. Yellow and green spheres represent different cations. The top left shows a range of "virtual" geometrically possible units and the top right shows the cations complexing the clusters and pulling certain structures out of solution. **See Color Plate 6.**

can alter the solution speciation affecting the outcome of the reaction.[1] This fact is exemplified in the assembly of reduced Mo clusters; ring shaped "Mo-Blues" and spherical shaped "Mo-browns", in which the building blocks *viz.* $\{Mo_1\}$, $\{Mo_2\}$, $\{(Mo)Mo_5\}$, $\{Mo_8\}$, that are formed in the reaction medium self-assemble to form very large molecular clusters of varying structural diversity ranging from balls, wheels, capped wheels and large "lemon" shaped clusters depending upon the specific reaction conditions.[6] However, the common aspect in these clusters is the "closed" nature of the structures being of spherical or toroidal in topology, and this aspect has been the subject of much discussion.[5]

From a crystal engineering point of view, one important factor that affects the formation of one particular POM species out of vast library of

candidates relates to the crystallization process itself. This point is brought into sharp focus when one realizes that, although many researchers focus on the POM framework exclusively, these POMs are poly-anions and cannot exist without the charge balancing cations, which often define the network into which the anion is "complexed" and electro-neutrality is achieved. In this way the cations themselves appear to be able to re-route or control the complex, since almost an infinite number of species and equilibria are available in solution that are removed from solution to the solid state (see Fig. 2). Since the properties of the cations such as size, charge, symmetry, solubility *etc.* are found to modulate the reactivity of POM building blocks, these cations can affect the nature of the product obtained from a POM synthesis.[7] A proper match between the cations and anionic POM species is needed for effective crystallization; hence most often the product isolated in crystalline form may not necessarily be the one with highest abundance in solution.[1h] Figure 3 depicts the distribution of cations, anionic POM clusters and their combined lattice arrangement in a true POM crystal structure, which highlights the vast number of counter cations that are present in the structure.

Modern crystal engineering is a hybrid of supramolecular chemistry and materials chemistry, dealing with the design and synthesis of

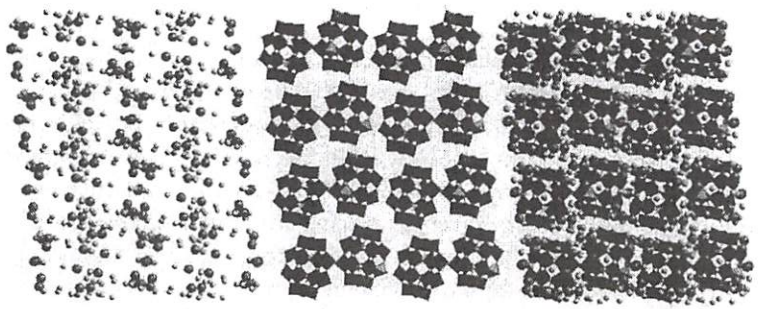

Fig. 3. Packing diagrams depicting the separate and combined arrangements of cations and POM cluster anions in a crystal lattice. *Left*: only cations (blue and green spheres) and solvent water molecules (rose spheres); *Middle*: only POM clusters (violet and yellow polyhedra) and *Right*: POM cluster anions, counter cations and solvent water molecules together in a crystal lattice. **See Color Plate 6.**

crystalline materials having the desired solid state properties. As POM chemistry is now very well established after several decades of research including intense underpinning structural studies, the initial structural and topological curiosity has been replaced by the quest for new tuneable and functional clusters capable of exhibiting novel, and controllable physical properties.[4] This means that the crystal engineering of POM-based materials should be directed towards the incorporation of well-conceived functionalities into such systems in order to develop the materials aspects of POM chemistry. For example POM synthesis, employing solution processing methods, has great potential to allow the assembly of new solid state materials using a molecular design approach.[9–12]

This chapter briefly outlines our recent efforts to control the self assembly of POM-based nanoscale molecules, and their assembly into nanostructures and solid state materials. Given that POMs are gigantic polyanions, the manipulation of the self-assembly process using cations is vital, and perhaps could provide the basis to design, using a crystal engineering type approach, pre-defined POM-based materials.[9] We reasoned that two things are most important here — first, the discovery of novel POM building blocks and second, the direction of their self-assembly in a controlled way to form useful materials. To achieve these targets, we are using a simple strategy, which is based on the use of bulky organic amine cations as counter-ions in POM synthesis.[9–12] The use of such bulky cations helps to isolate self-assembled POM species in one-pot reaction systems thus preventing their rapid aggregation into clusters having stable uniform spherical topology. Also such cations together with other linker units are found to be capable of directing the self-assembly of POM building blocks into extended structures. We termed this approach as "Shrink wrapping"[9–12] and involves mainly the use of organic amines such as hexamethylene tetramine (HMTA), triethanol amine (TEA), *N,N*-bis-(2-hydroxyethyl)-piperazine (BHEP), morpholine etc. which are capable of acting as well defined (encapsulating) cations, as well as ligands (although at low pH it is unlikely these amines act as ligands), buffers, and even as redox reagents in some cases (see Scheme 1). Further, we were able to produce a number of discrete iso- and heteropolyoxo clusters as well as many extended architectures using this simple but efficient concept, described briefly in the following sections.

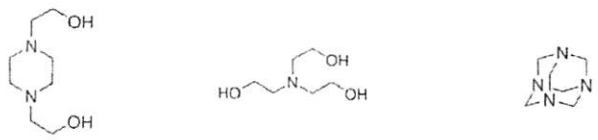

Scheme 1. The various shrink-wrapping cationic precursors used in our studies.[9–12]

1.1. *Background*

The effective control over the self-assembly of $\{MO_x\}$ units in the traditional "one-pot" synthesis has always been the main aim for researchers looking for new POM clusters. In the case of reduced Mo-based clusters often called "Mo-blues", the work of Müller *et al.* showed that it was possible to generate and control the self-assembly of some building units in solution by varying the synthetic conditions.[5] One of such building block is the pentagonal $\{Mo(Mo)_5\}$ unit which is pivotal in the effective tiling of many spherical Archimedean solid structures. These $\{Mo(Mo)_5\}$ building blocks, in the presence of suitable linkers, such as doubly bridging $\{MoV_2O_4(ligand)\}$ units, where "ligand" can be acetate, sulfate etc., leads to giant mixed-valence clusters with diverse topologies such as the spherical icosahedral $\{Mo_{132}\}$, big wheel $\{Mo_{154}\}/\{Mo_{176}\}$, capped cyclic $\{Mo_{248}\}$ and basket shaped $\{Mo_{116}\}$ architectures[5,6] (Fig. 4). One other important achievement with Mo-based clusters, in the context of cluster engineering, is the ability to manipulate the structure, pore size and interior properties of the spherical Keplerate capsules by changing the bidentate ligands of the $\{MoV_2O_4(ligand)\}$ linker.[13] In parallel with these studies in "Mo-blue" chemistry, Pope and co-workers have achieved interesting W-based clusters including the largest tungstate cluster reported so far, by using hetero-transition metal ions as linkers.[14] Apart from Mo and W, which are the two main metals explored in POM chemistry, the engineering of novel cluster types based on other metals like vanadium,[15] tantalum,[16] niobium,[17] uranium[18] and palladium[19] is also being explored with great vigor since these represent possible new routes in the search for new metal-oxide based materials. Further, the pentagonal

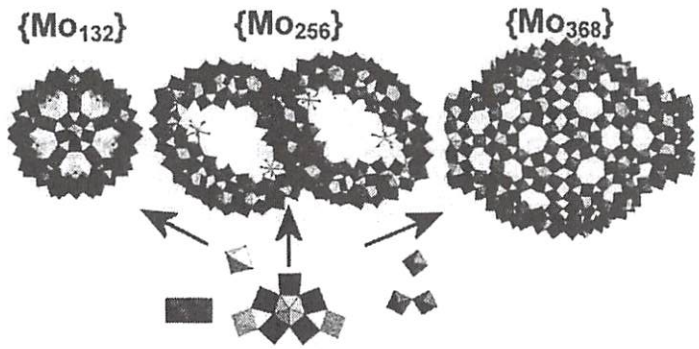

Fig. 4. $\{Mo_1\}$, $\{Mo_2\}$, $\{(Mo)Mo_5\}$ etc. building blocks self-assemble according to the reaction conditions leading to various structurally diverse Mo-blue clusters.[5,6] **See Color Plate 7.**

$\{M(M_5)\}$ building block necessary for the tiling of large Archimedean structures, was recently discovered in the case of W and Nb clusters (rather than just Mo),[20] pointing to the prospect of the isolation of large clusters similar to "Mo-blues" in the case of these metals as well.

The often serendipitous nature of the "one-pot" reactions has prompted researchers to utilize a better defined "building block approach", which utilizes preformed POM clusters as building blocks for the generation of networks or aggregates.[1,4] In this way, POM building blocks are assembled either through M–O–M oxo bridges or by the use of metal–organic complexes as linkers. In fact an almost bewildering number of molybdenum and tungsten oxide-based organic–inorganic hybrid materials are reported by various groups using metal–organic complexes/coordination polymers as linkers between POM clusters, and the number of examples is expanding seemingly at an exponential rate.[21] The metal organic units used as linkers can also act as charge balancing counterions, templates and covalently linked network constituents in these compounds. However, the multiplicity of coordination sites on POM building blocks often makes the product prediction difficult using a "building-block approach" as well similar to the "one-pot" synthetic approach. Further, most of these studies exploit well known clusters and have not led to profoundly new or highly functional materials with new properties. However, many of the reaction

systems in this class have used hydrothermal reaction conditions, which has led to some interesting results and new materials that appear to cause a shift in their reactivity from the kinetic to the thermodynamic domain compared to traditional aqueous reactions, such that the equilibrium phases are replaced by more complex metastable phases.[22] Therefore, the hydrothermal method is now commonly employed for the engineering of organic–inorganic hybrid POM materials as a modification of "one-pot" synthesis. Many interesting architectures and frameworks are engineered through hydrothermal synthesis by the careful selection of the metal organic and POM building blocks.[23]

Functionalization of POM clusters with organic units, *via* ion exchange or by direct covalent attachment, is another important strategy towards the development of functional materials as it will enhance the synergistic combination of properties of the polyoxometalates and organic units. By tailoring the organic and/or inorganic part properly, one could design interesting hybrid systems with unique functional properties not normally available in the component parts.[24]

1.2. *Isopolyoxometalates and their derivatives*

Isopolyoxometalates (iso-POMs) are a sub-class of polyoxometalates, which are composed of a metal-oxide framework, but without an internal heteroatom/heteroanion template. As the POM clusters are synthesized by the condensation of $\{MO_x\}$ units (where M = Mo,W; $x = 4 - 7$) at low pH, a number of possible edge and corner-shared $\{MO_x\}$ intermediates are possible, which can then serve as structural components of large polyoxometalates assembled by conservative self-organizing processes. However, it is observed that the self-organization of these building blocks to large structures often requires a template to assemble the cage around, such as a heteroanion, e.g. PO_4^{3-}, thus leading to the formation of heteropolyanions. Because of this, the number of POM structures formed without the templating effect of an heteroanion/heteroatoms is surprisingly limited. For example, compared to the vast class of known heteropolytungstates, only a limited number of isopolytungstates have been reported thus far.[4] It is noted that, solution control by the manipulation of pH as well as cations are very important in the synthesis of iso POMs, and perhaps define an

even more interesting target than the heteropolyanions for the use of crystal engineering techniques to control the cluster and crystal architectures.

The use of bulky organic cations to control the self-assembly of building blocks in the synthesis of iso-POMs was successfully leading to the development of a new family of Mo-based iso-POMs. By utilizing protonated hexamethylenetetramine (HMTAH, $C_6H_{13}N^{4+}$) as counterion, the cluster compound $(HMTAH)_{10}[H_2Mo_{16}O_{52}]\cdot 34H_2O$, $\{Mo_{16}\}$, was isolated as crystalline precipitate from an acidified molybdate solution (pH 4) in the presence of a reducing agent in 20–30% yield.[9] This cluster has a "flat" geometry and four of the sixteen Mo centers are one-electron reduced. The main body of this "bat-shaped" cluster consists of a central unit with 12 molybdenum atoms and two "wings" each with two molybdenum atoms (giving the formulation $[\{Mo_{12}\} + 2\{Mo_2\}]$). The role of the "shrink-wrapping" cation in the encapsulation of this rare non-spherical POM can be understood from the very close interaction between surface oxoligands of the cluster anion and the HMTAH cations. There are 18 short hydrogen-bonded cluster surface oxygen-to-cation interactions for the anion. This means that the clusters are extensively linked to the HTMAH cations *via* hydrogen bonds. Also, the anion layers in this compound are effectively separated from each other by HMTAH cation layers. Figure 5 clearly illustrates that the cluster anions are effectively covered, or

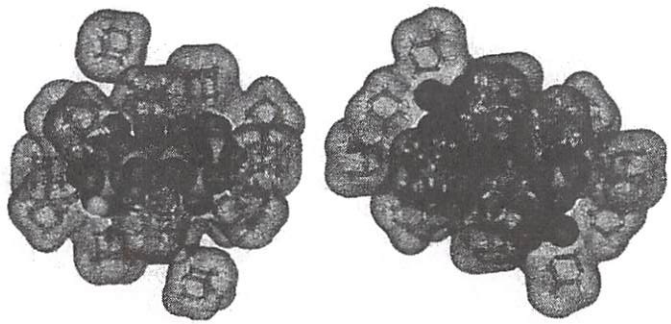

Fig. 5. Model for an actual crystal structure of a POM. The $\{Mo_{16}\}$ isopolyoxometalate cluster anion is closely surrounded by HMTAH cations, effectively "shrink-wrapping" around it.

"shrink-wrapped" by the HTMAH cations in the solid state. Although cation–anion association will be present in solution, encouraged by both electrostatic and hydrogen-bonding effects, the extent of the interactions seen in the present compound in solid state appears to play a crucial role in solution as well. This is because experiments attempting to synthesize the $\{Mo_{16}\}$ cluster under similar reaction conditions (by altering pH value, concentrations, ionic strength, and temperature), but with different large cations (for example $[HN(CH_2CH_2OH)_3]^+$), resulted in the formation of the well-known Dawson-type cluster. Also attempts to dissolve this compound in the presence of other cations appear to result in the decomposition of the cluster anions. These observations strongly support the "Shrink-wrapping" effect of the bulky organic cation HMTAH in the formation of this iso-POM.

This $\{Mo_{16}\}$ cluster anion possesses high nucleophilicity and hence can bind two divalent transition-metal ions (such as Fe^{II}, Mn^{II}, Co^{II}, Ni^{II}, or Zn^{II}) to its framework. This led to a family of isostructural complexes exhibiting the basic topology found for the parent $\{Mo_{16}\}$ cluster with the addition of two $[M^{II}(H_2O)_4]$ moieties yielding a complex of the composition: $[M^{II}_2(H_2O)_8H_2Mo^{V}_4Mo^{VI}_{12}O_{52}]^{6-}$ (M = Mn, Fe, Co). The encapsulating effect of the "shrink-wrapping" cations is found to prevent any significant inter-cluster magnetic exchange interactions in these compounds.[25] The extension of the "Shrink-wrapping" organic cation strategy to tungsten-based systems has resulted in the trapping and isolation of an interesting isopolytungstate $(TEAH)_6Na_2\{(H_2O)_4K[H_{12}W_{36}O_{120}]\}\cdot 17H_2O$, which is the largest isopolytungstate reported so far in the literature.[26] This cluster compound was isolated from a reaction mixture comprising Na_2WO_4, $Na_2S_2O_4$ and protonated triethanolamine (TEAH) as organic cation, in water at pH 2. Subsequent experiments have shown that the addition of $Na_2S_2O_4$ is not necessary for the synthesis of this compound. The 3-fold symmetric cluster anion $[H_{12}W_{36}O_{120}]^{12-}$,$\{W_{36}\}$, is comprised of three $[H_4W_{11}O^{38}]^{6-}$, $\{W_{11}\}$, cluster subunits linked together by three $\{WO_6\}$ bridges. The center of this "Celtic ring" cluster has a $\{W_6O_6\}$ ring, that maps extremely well onto the structure of the crown ether 18-crown-6 and holds a K^+ ion at its center.

Focusing on the crown ether like central cavity of $\{W_{36}\}$ cluster anion for host–guest chemistry with alkali and alkali-earth metal ions, complexes of the type $\{MW_{36}\}$ ($M = K^+$, Rb^+, Cs^+, NH_4^+, Sr^{2+} and Ba^{2+}) have been

successfully synthesized.[27] These complexes demonstrate that, $\{W_{36}\}$ cluster anion can act like a type of inorganic "crown ether" with similar preferences to 18-crown- 6, but with much greater rigidity, and therefore, having the potential to distinguish between different cations. In a further extension of this work, a range of protonated aliphatic and aromatic guest cations such as 2-phenethylamine, 4-phenylbutylamine, *p*-xylylene diamine and 1,6-diaminohexane were successfully locked into the crown-ether like cavity of this iso-POM, and their structure directing effects on the resulting framework arrangements are probed. It was found that parts of the organic guest cation protrude from the central binding cavity of the cluster and that the nature of this protruding organic "tail" has a directing ability and is in fact able to control the solid-state structure of the resulting compounds (see Fig. 6).[28]

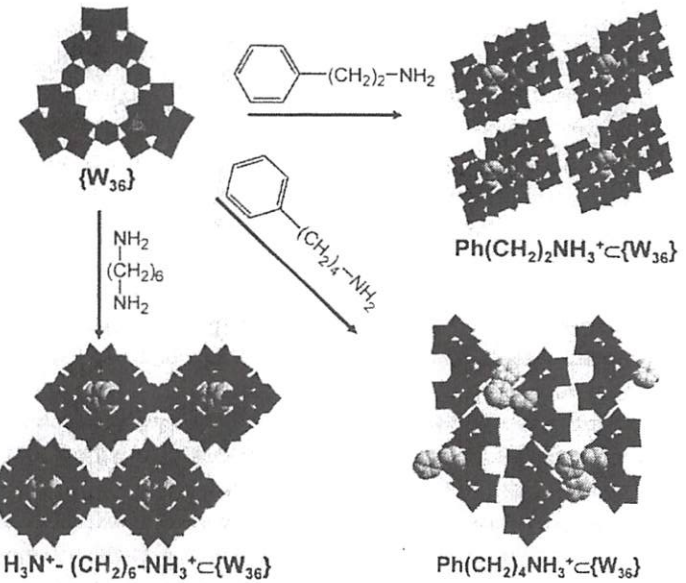

Fig. 6. Illustration of the framework arrangement of some host guest complexes prepared from inorganic crown ether analogue $\{W_{36}\}$ cluster and various amines. The effect of protruding amines in directing the self-assembly leading to various framework arrangements can be visualized from these projections. All the frameworks are viewed along crystallographic a axis.

The synthesis of $\{W_{36}\}$ cluster showed that the presence of inorganic species such as $Na_2S_2O_4$ in the reaction medium could be crucial in the isolation of similar isopolytungstates. But unlike the isopolymolybdates, the influence of such inorganic species on the assembly of isopolytungstates has not been well-documented in the literature. In an attempt to discover radically new cluster architectures in the isopolytungstate family, we have found that, acidification of a solution of sodium tungstate to pH 3.4 in presence of $Na_2S_2O_4$ could lead to the isolation of a "S"-shaped $[H_4W_{22}O_{74}]^{12-}$ cluster anion, $\{W_{22}\}$, and on lowering the pH further (down to pH 2.4) could also lead to a related "§"-shaped $[H_{10}W_{34}O_{116}]^{18-}$ cluster anion, $\{W_{34}\}$.[29] It is noteworthy that we have also observed that these new isopolytungstates could only be isolated in good yield in the presence of the inorganic species Na_2SO_3, even though it is not included in the crystal structure.

All of the above isopolytungstates $\{W_{36}\}$, $\{W_{34}\}$ and $\{W_{22}\}$ contain a basic building block: $\{W_{11}\}$ ($[H_4W_{11}O_{38}]^{6-}$), having a fish-net structure, in which two fused half cubanes share one edge with another half cubane, and has two corner-shared dimeric tungsten-species bridging them together. In $\{W_{36}\}$ cluster, these $\{W_{11}\}$ subunits are linked together by three $\{WO_6\}$ units to give the celtic ring shaped cluster having a crown-ether type cavity at the center. In the $\{W_{22}\}$ cluster, two $\{W_{11}\}$ building units are directly linked together to give the "S" shaped cluster, while in the $\{W_{34}\}$ cluster, two identical $\{W_{11}\}$ subunits are connected together in a *trans* fashion by a $[H_2W_{12}O_{42}]^{10-}$, $\{W_{12}\}$ unit through two μ_2-oxo bridges to give an expanded "§"-like architecture. The evolution of the clusters from $\{W_{11}\}$ to $\{W_{22}\}$, $\{W_{34}\}$ and $\{W_{36}\}$ is very important (Fig. 7), as it leads towards a new building block principle for developing new clusters of isopolytungstates. It should be noted here that, unlike the $\{W_{36}\}$ cluster, the $\{W_{22}\}$ and $\{W_{34}\}$ clusters are formed without the presence of any shrink wrapping cations. But it is intriguing to observe that the approximately C_{3v} symmetric $\{W_{36}\}$ cluster anion is formed in the presence of shrink-wrapping cation TEAH having approximately C_{3v} symmetry, the absence of which led to the formation of linear structures such as $\{W_{22}\}$ and $\{W_{34}\}$. This observation could be pointing to the structure directing role of the "shrink-wrapping" cations in the synthesis of such iso-POM species.

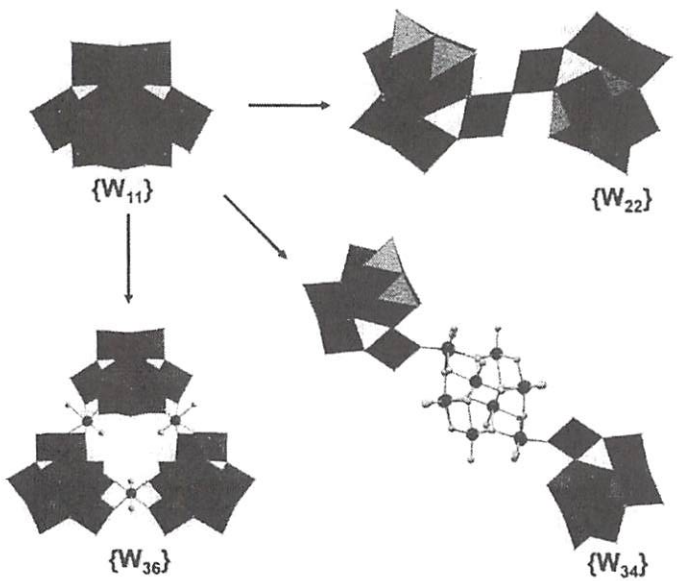

Fig. 7. Formation of three isopolytungstate formed by the different linking modes of same basic building block $\{W_{11}\}$. $\{WO_6\}$ units (violet polyhedra), W, (violet spheres), O (rose spheres). **See Color Plate 7.**

"Shrink-wrapping" cations could also lead to isopolytungstates that are structural analogues of heteropoly acids. For example, a reaction system comprising tungstates and TEAH cations at lower pH values (around 0.8) yielded a fundamentally new type of isopolytungstate isolated as $(TEAH)_6[H_4W_{19}O_{62}]$, $\{W_{19}\}$.[30] This Dawson structural archetype incorporating a $[WO_6]^{6-}$ anion template is a rare and unprecedented cluster type. Furthermore, the stabilization of the $\{WO_6\}$ moiety in a trigonal prismatic coordination environment was new in polytungstate chemistry. In the absence of the bulky organic TEAH cations, under otherwise identical reaction conditions, only the well known $[W_{10}O_{32}]^{4-}$ cluster compound was formed, therefore implying the existence of a crucial cation effect on the formation of this new isopolytungstate.

2. Host-Guest Chemistry to Networks

2.1. *Cage compounds and switchable POMs*

Many POM clusters can be thought of as molecular cages enclosing some particular species at its center. For instance the conventional Dawson archetype incorporates two tetrahedral anions such as PO_4^{3-}, AsO_4^{3-}, or SO_4^{2-} at the center, while the Keggin clusters incorporate only one such anion. Incorporation of a redox-active species inside a POM cage would be highly desirable in this respect, in view of the development of switchable POM molecules. In an attempt to develop a POM based switchable system, we targeted the incorporation of some non-conventional templating units, e.g. sulfite ions, inside a Dawson cage. The hypothesis for this investigation was that the confinement of such species in a closed molecular cage could lead to properties arising from the intra-molecular electronic interactions between the encapsulated anions. Moreover, this could also lead to the manipulation of the physical properties of the $\{Mo_{18}\}$ Dawson type POM cluster. The incorporation of two sulfite ions as templating moieties inside a Dawson-like cluster is achieved from a reaction mixture at pH 4.0 containing metal salts, excess of protonated triethanolamine (TEAH) cations and $Na_2S_2O_4$ as a reducing agent as well as the source of SO_3^{2-}.[10] The product is crystallized as $(TEAH)_6[Mo_{18}O_{54}(SO_3)_2]\cdot 4H_2O$ which incorporates two pyramidal sulfite SO_3^{2-} ions as the central cluster templates.

This new cage compound represents the first Dawson-like $\{M_{18}\}$ cluster incorporating the pyramidal sulfite anion, and the first that includes two such pyramidal anions in the same $\{M_{18}\}$ cage. The two sulfite anions show a short S–S interaction inside the cluster cage and hence unusual electronic properties. This new "non-classical" Dawson-like cluster also shows interesting thermochromic behavior between 77 K (pale yellow) and 500 K (deep red). In an extension of this approach, the first two examples of polytungstate clusters incorporating two sulfite anions, $(TBA)_4[W^{VI}{}_{18}O_{54}(SO_3)_2]$ and $K_7Na[W^{VI}{}_{18}O_{56}(SO_3)_2(H_2O)_2]\cdot 20H_2O$ have been successfully synthesized, where TBA = tetrabutylammonium cation.[31] The cluster $K_7Na[W_{18}O_{56}(SO_3)_2(H_2O)_2]\cdot 20H_2O$ has a curious structure incorporating two terminal water ligands which was unknown for a

closed-shell hetero-polyoxometalate cluster (HPOM clusters) of any type. Moreover, this compound demonstrated new electronic properties. The cluster anion, $[W_{18}O_{56}(SO_3)_2(H_2O)_2]^{8-}$, undergoes a unique electron-transfer reaction when heated, in which a structural re-arrangement allows the two embedded pyramidal sulfite (SO_3^{2-}) anions to release up to four electrons (analogous to the "soldiers" hidden inside the "Trojan Horse") to the surface of the cluster generating the sulfate-based, deep blue, mixed valence cluster $[W_{18}O_{54}(SO_4)_2]^{8-}$. Although electron-transfer reactions and structural rearrangements are well-known for hetero-POMs, this is the first example of a coupled structural rearrangement and electron-transfer process, whereby the electrons are "released" from the core of the cluster. It is also the first example of a fully characterized unimolecular reaction involving an HPOM.

The successful trapping of one $\{WO_6\}$ unit inside a Dawson-like cage leading to the formation of the iso-POM $(TEAH)_6[H_4W_{19}O_{62}]$ suggested the possibility of replacing the central $\{WO_6\}$ moiety of this system with other similar $\{XO_6\}$ species, for example X = Pt^{IV}, Sb^{V}, Te^{VI}, or I^{VII}. Encapsulation of such templates in very high or very low oxidation states should significantly affect the acidic, catalytic, and redox properties of the resulting cluster systems. Following a synthetic strategy similar to that of the $\{W_{19}\}$ iso-POM, we were able to embed iodine(VII) into a Dawson-like $\{W_{18}O_{54}\}$ matrix as the periodate species IO_6^{5-} to yield a range of cluster salts, $K_6[H_3W_{18}O_{56}(IO_6)]\cdot 9H_2O$, $(TPA)_6[H_3W_{18}O_{56}(IO_6)]$, and $(TBA)_6[H_3W_{18}O_{56}(IO_6)]$, (TPA = tetrapropylammonium cation).[32] The formation of $[H_3W_{18}O_{56}(IO_6)]^{6-}$ appears, at least empirically, to be induced by the IO_6^{5-} anion (which contains a three-fold symmetric axis), although the cluster is produced in a modest yield. Prompted by this observation, we undertook the synthesis of $[H_3W_{18}O_{56}(IO_6)]^{6-}$ in the presence of three-fold symmetrical TEAH cation, and obtained $(TEAH)_6[H_3W_{18}O_{56}(IO_6)]$ in higher yields. This result is in tune with our previous observations that the formation of 3-fold symmetrical $\{W_{19}\}$ cluster, $[H_4W_{19}O_{62}]^{6-}$, requires the presence of three-fold symmetrical TEAH cations (the well-known $[W_{10}O_{32}]^{4-}$ cluster is formed in the absence of TEAH)[30] and hence highlights the cation effect in the formation of these POM cage clusters.

Looking for other non-conventional switching systems, we also targeted the encapsulation of TeO_6^{6-} units within $\{W_{18}O_{54}\}$ cluster shells to give a tellurate-based Dawson-like anion.[33] Unlike our previous experiences, this did not appear to be straightforward, and necessitated techniques such as cryospray mass spectroscopy (CSI-MS) to screen the reaction systems for suitable cations. Of the cations screened, dimethylammonium (DMAH) and tetrabutylammonium (TBA) were found to be successful, yielding the Te^{VI}-encapsulated Dawson-like cluster anion $[H_3W_{18}O_{56}(Te^{VI}O_6)]^{7-}$ as $Na(DMAH)_6[H_3W_{18}O_{56}(Te^{VI}O_6)]\cdot 14H_2O$ and $(TBA)_7[H_3W_{18}O_{56}(Te^{VI}O_6)]\cdot 4CH_3CN$ respectively. We also investigated the redox properties of $[H_3W_{18}O_{56}(Te^{VI}O_6)]^{7-}$ to see if it was possible to access a Te^{IV}-based species by reducing the inner hetero atom. On addition of solid $Na_2S_2O_4$ to the acidified solution of $[H_3W_{18}O_{56}(Te^{VI}O_6)]^{7-}$, the solution initially turned blue, owing to the reduction of the $\{W_{18}\}$ based cluster shell, and then became pale yellow within seconds. We postulated that the central Te was reduced in this process from Te^{VI} to Te^{IV}. This reduction was confirmed by the isolation of $[H_3W_{18}O_{57}(Te^{IV}O_3)]^{5-}$, by precipitation with TBA, and this material on crystallization from acetonitrile followed by single-crystal X-ray diffraction analysis revealed that the Te^{IV} center shifts by 1.10 Å towards one end of the cluster to form a pyramidal tellurite ion, see Fig. 8. Hence, upon formal two-electron reduction, the

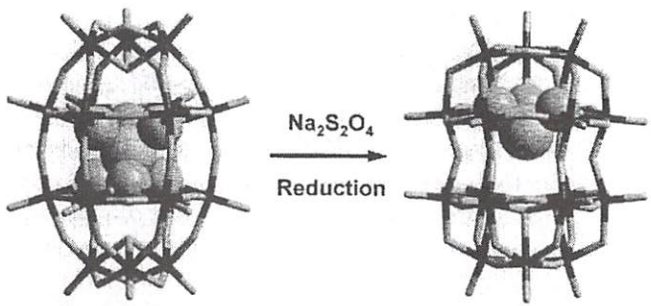

Fig. 8. Structural transformation as a result of the reduction of Te^{VI} to Te^{IV} inside a tungsten based molecular cage. **See Color Plate 8.**

central octahedral $\{Te^{VI}O_6^{6-}\}$ unit is transformed into a pyramidal $\{Te^{IV}O_3\}^{2-}$ unit with the breaking of three Te–O bonds. Two interior "capping" oxo ligands were also lost during this reduction process. This redox reaction can be monitored *in situ* by the use of CSI-MS analyses. Further, it was observed that the inclusion of the tellurium-based heteroanion activates the surface of the $\{W_{18}O_{54}\}$ cluster cage, facilitating the assembly of the clusters to nanoscale structures without the introduction of other transition metal electrophiles. The self-assembled nano structure thus isolated in the solid state, $Na_8(DMAH)_{18}[H_{10}Te^{VI}_2W_{58}O_{198}]\cdot 35H_2O$, contains two $\{W_{18}Te^{VI}\}$ anions linked together by two $\{W_{11}\}$ units.

The role of cations is found to be important in the isolation of the above Te-based clusters as well. $Na(DMAH)_6[H_3W_{18}O_{56}(Te^{VI}O_6)]\cdot 14H_2O$ is achieved from a reaction system containing Na_2WO_4 and $Te(OH)_6$ at pH 0.8 in the presence of DMAH. The presence of DMAH is crucial since its absence leads exclusively to the formation of the Anderson-type cluster $[TeW_6O_{24}]^{6-}$, which reiterates the pivotal role of organic cations for the assembly of new POMs.[3] Inclusion of other transition metal based hetero anions as templates inside a Dawson-like cage has also been attempted. This has been achieved in the case of mixed metal (V/Mo and V/W) Dawson-like capsules having a unique composition $\{M_{17}V_3\}$.[34] A family of clusters which can be formulated as $V_2A\{M_{17}V_1\}$ having the α-Dawson cluster framework have been synthesized and the synthetic approach involves the aqueous reaction of $Na_2MO_4\cdot 2H_2O$ (M = Mo or W) and NH_4VO_3 in presence of protonated triethanolamine (TEAH) as "shrink-wrapping" cation. A variety of experimental techniques have been tested to synthesize these compounds including hydrothermal synthesis. It is interesting to note that in all these cases, each of the $\{M_{17}V_3\}$ cluster anions obtained contain two $\{V^VO_4\}$ vanadate templates with one $\{V^{IV}O\}^{2+}$ vanadyl group integrated into the $\{M_{18}\}$ cluster framework. Figure 9 shows a series of Dawson-like cluster cage compounds developed in our group so far incorporating various guest species.

2.2. *POM based architectures and framework materials*

The last couple of decades have witnessed an enormous growth of open framework inorganic materials. The majority of these include metal–organic frameworks containing discrete inorganic building blocks; the

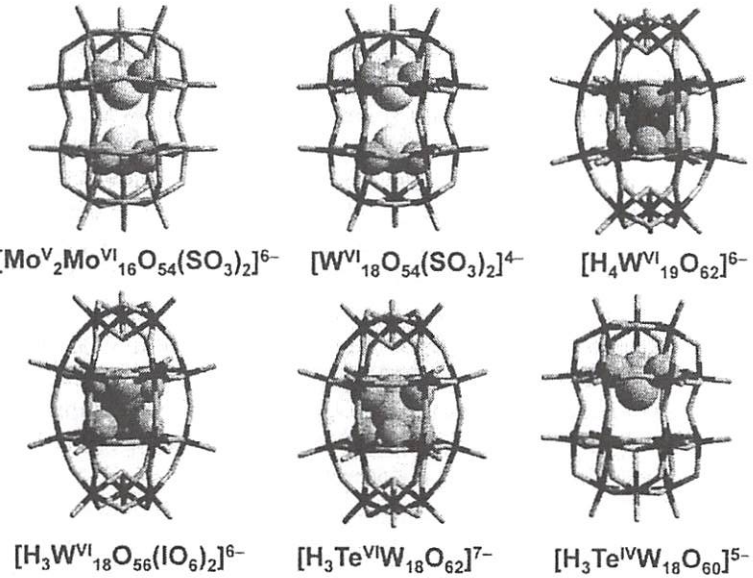

Fig. 9. Some of the Dawson-type cage compounds developed in the Cronin group incorporating various guest systems.

geometry and cavities of such frameworks mainly depending on the nature of the building units.[35] Often, POM clusters are used as large inorganic building blocks in an attempt to expand the lattice of such framework materials.[36] In this respect, we have successfully combined the "shrink-wrapping" strategy and "building block approach" with the help of suitable linker units resulting in diverse polymeric architectures and robust framework materials based on some well-known POM building blocks. For instance, we have utilized silver(I) to act as a linker in POM chemistry due to its versatile range of geometries and bonding modes.[37] In this way, using β-octamolybdate as building unit and bulky TBA as cations, two 1D chain structures, $(TBA)_{2n}[Ag_2Mo_8O_{26}]_n$ and $(TBA)_{2n}[Ag_2Mo_8O_{26}(CH_3CN)_2]_n$ have been formed by the condensation with Ag^{I} salts.[11] In these 1D chains, the flexible TBA cations nearly completely wrap around the linear chain of linked $[Ag^{I}Mo^{VI}_{8}O_{26}Ag^{I}]^{2-}$ units effectively isolating them from one another. The mode in which the $\{Ag(Mo_8)Ag\}$-type "units" assemble to create the overall solid state architecture was also found to be critically dependent on

the reaction conditions. On changing the cations from TBA to small cations, the steric shielding and/or "shrink-wrapping" ability of organic cations is reduced leading to a partial disruption of the "insulation" and as a result, the electrophilic polymolybdate chains could be interlinked. This leads to a grid-like structure $(TBA)_{2n}[Ag_2Mo_8O_{26}(DMSO)_2]_n$ and a 2D array, $(HDMF)_n[Ag_3(Mo_8O_{26})(DMF)_4]_n$, where DMSO = dimethylsulfoxide and HDMF = protonated dimethylformamide. In the latter, the relatively bulky TBA ions are exchanged for HDMF cations thereby allowing the chains to condense to a 2D array. Interestingly, the use of Ph_4P^+ ions instead of TBA cations leads to a discrete cluster $(Ph_4P)_2[Ag_2Mo_8O_{26}(DMSO)_4]$. These compounds clearly demonstrate that suitable combination of linkers and bulky organic cations can effectively control the self-assembly of POM building blocks thereby resulting in interesting architectures (see Fig. 10).

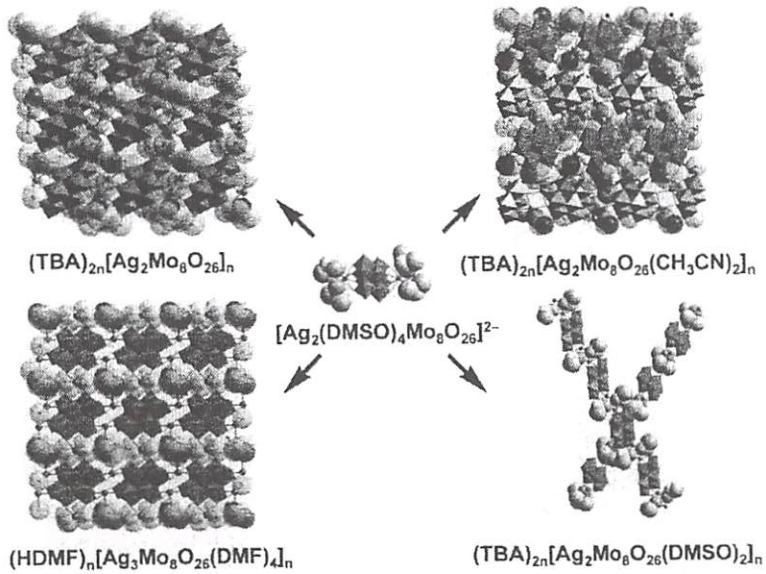

Fig. 10. Summary of the structures isolated from the silver-octamolybdate reaction system. The solvents and counterions are represented in space fill models to highlight their influence in determining the overall topologies achieved which include monomeric structures, 1D chains, grid and 2D network as shown. Color scheme: $\{Mo_6\}$ polyhedra orange, O (rose), C (grey), N (blue), S (yellow). **See Color Plate 8.**

Further studies on silver-octamolybdate systems by varying solvents and counter ions led to a new set of interesting POM architectures.[38] In these structures, formation of $\{Ag_2\}$ linking units is realized and the fine-tuning of Ag–Ag distances in these linkers is achieved with the help of different coordinating solvents. Five compounds based on silver octamolybdate building blocks have been isolated, including an uncommon 0D $(Ph_4P)_2[Ag_2(CH_3CN)_2(Mo_8O_{26})]$, three 1D polymeric chains $([Ag(C_7H_{12}O_2N)(CH_3CN)]_{2n}$ $[Ag_2(CH_3CN)_2(Mo_8O_{26})]_n \cdot 2CH_3CN$, $(Ph_4P)_{2n}[Ag_2(DMF)_2(Mo_8O_{26})]_n \cdot 2DMF$, and $(DMAH)_{2n}[Ag_2(DMF)_2(Mo_8O_{26})]_n \cdot 2DMF$, and a 2D cross-linked network $[(Ag(DMF))_2(Ag(DMF)_2)_2Mo_8O_{26}]_n$. Figure 11 depicts some of these architectures highlighting the crucial role of counter ions and solvent molecules in the isolation of such architectures. Therefore, these studies on silver-octamolybdate systems comprehensively describe the

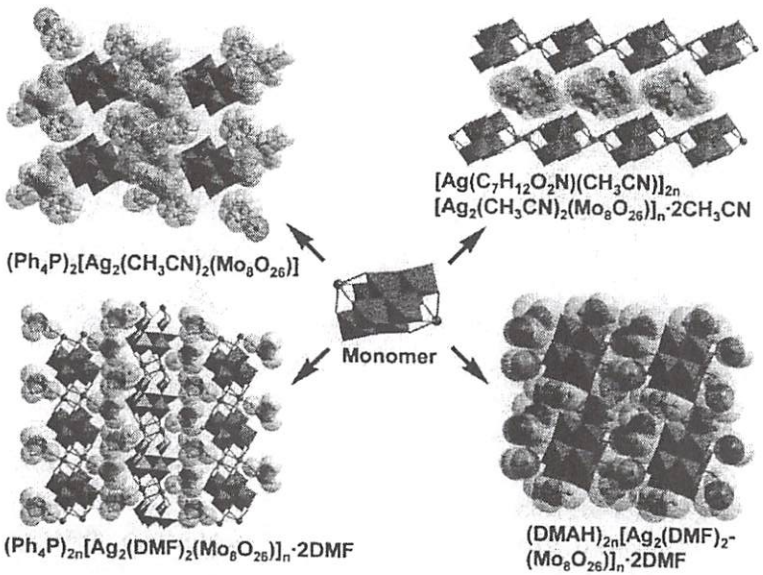

Fig. 11. More examples of silver-octamolybdate based architectures isolated as a result of solvent and counter ions influencing self-assembly. Color scheme: $\{Mo_8\}$ polyhedra (orange), O (rose), C (grey), N (blue), P (pink). **See Color Plate 9.**

synthetic strategies that allow the formation of 0D, 1D and 2D structural assemblies starting from a single POM building block $\{Mo_8\}$, and the flexible silver(I) cation linker.

The above studies on silver-octamolybdate systems have also shown that, careful control over solvent and ligand systems can result in the formation of structurally supporting $\{Ag_2\}^{2+}$ building blocks. Exploiting the potential of such silver(I) dimers to act as linkers between larger isopolyoxometalates, we were able to develop a purely inorganic 3D porous framework.[39] The resulting "POM based open framework" or "POMOF", $[Ag(CH_3CN)_4]A\{[Ag(CH_3CN)_2]_4[H_3W_{12}O_{40}]\}$, is made up of two principal SBUs, protonated α-metatungstate clusters $[H_3W_{12}O_{40}]^{5-}$ ($\{W_{12}\}^{5-}$) and dimeric $\{[Ag(CH_3CN)_2]_2\}^{2+}$ ($\{Ag_2\}^{2+}$) bridging units. These building units are assembled such as to enclose two sets of collinear channels in the crystal lattice. *Td*-symmetric $[Ag(CH_3CN)_4]^+$ units are located in these channels and appear to act as templates in the self-assembly of this framework material. One important key to this framework formation is the ability of the Ag^+ to self-organize into $\{Ag_2\}^{2+}$ dimers with short silver–silver contacts which are stabilized by argentophilic metal–metal interactions. Each dimeric $\{Ag_2\}^{2+}$ motif cross-links four POM building blocks. It was observed here that, in order to encourage the formation of the Ag…Ag interactions, coordinating solvents must be avoided, because the use of such solvents resulted in the capping of Ag centers yielding low dimensional structures. This material shows reversible sorption capabilities allowing the sorption and desorption of small organic molecules. The assembly of such purely inorganic POM-based porous frameworks is highly desirable in materials science, because they are expected to combine the thermodynamic stability of zeolites and mesoporous silicas with the sophistication and versatility of metal–organic frameworks (MOFs).

The effect of the structural features of the organic cations on the supramolecular structure of the POM framework is examined in the case of polyoxomolybdenum(V) phosphate clusters $[CH_6N_3]_{12}[Mo_{12}O_{62}H_{11}NaP_8] \cdot 11H_2O$, $[C_4H_6N_3]_{14}[Mo_{12}O_{62}H_9NaP] \cdot 13H_2O$ and $[C_2H_{10}N_2]_6[Mo_{12}O_{62}H_9Na_3P_8] \cdot 18H_2O$ containing sodium-linked dimeric $\{Mo_6\}_2$ moieties as inorganic building blocks and guanidinium, 2-aminopyrimidinium or protonated ethylenediamine respectively as structure-directing amine cations.[40] It was found that in these compounds, the rigid amines guanidinium and

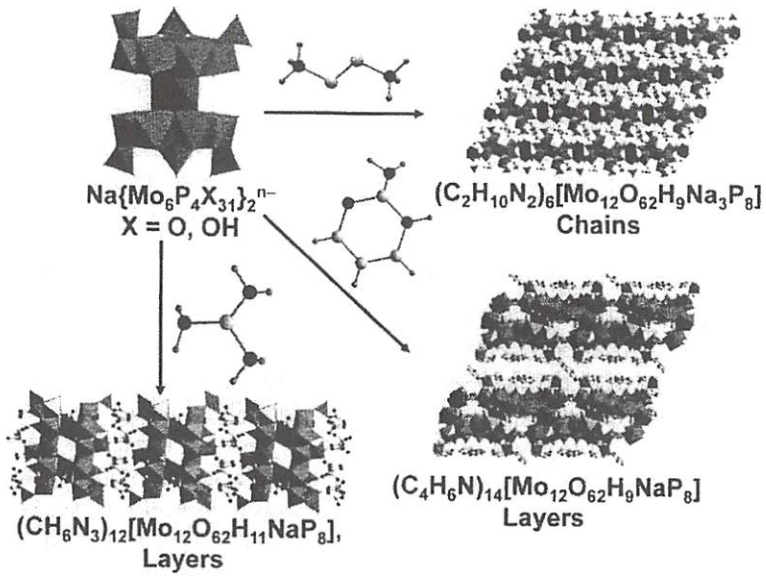

Fig. 12. Summary of the formation of layered or chain-like structures from $\{Mo_6\}_2$ moieties depending on the amine used in the synthesis.

2-aminopyrimidinium induced the formation of layered arrangements, whereas structurally more flexible ethylenediamine resulted in the formation of polymeric chains, Fig. 12. This study is therefore one of the best examples which shows that the geometry, rigidity and hydrogen bonding ability of organic amine cations can influence the overall structure of the POM supramolecular framework.

The transfer of properties from small building blocks to the large POM cluster assemblies is an interesting aspect in POM chemistry that is ripe for expansion/concrete development. For example, Craig Hill and coworkers have achieved chirality transfer from smaller enantiopure organic molecules such as tartrate onto POM clusters leading to chiral, nonracemizing and enantiomerically pure polytungstate clusters.[41] Extending this concept into large POM based supramolecular frameworks, we have successfully developed a chiral framework material having sorption

capabilities. We used diprotonated (2)-sparteine as the chiral cation and the dimeric polyoxomolybdenum (V) phosphate anion $[H_{15}Mo_{12}NaO_{62}P_8]^{8-}$ as the POM building block, resulting in the porous chiral hybrid framework $(C_{15}H_{28}N_2)_4(C_9H_6O_6)_1[H_{15}Mo_{12}NaO_{62}P_8]\cdot 10H_2O$.[42] In this chiral framework, each dimeric $\{Mo_6\}$ POM cluster is shielded by four (2)-sparteine cations which form N–H···O hydrogen bonds to the cluster anion (minimum distance dN–H···O = 2.67 Å). The structure is further reinforced by a complex network of hydrogen-bonded water molecules and incorporates chiral channels along the crystallographic a axis, capable of accommodating organic molecules like benzene tricarboxylic acid and water molecules. The porous nature of this compound is confirmed by reversible water sorption properties.

In our attempt to develop POM based chiral frameworks, we have also used large chiral metal–organic macrocation as one of the starting material. Fe-acrylate based chiral macrocation $[Fe_3(\mu_3\text{-}O)(CH_2\ CHCOO)_6(H_2O)_3]^+$ is reacted with trilacunary Dawson cluster $[a\text{-}P_2W_{15}O_{56}]^{12-}$, $\{P_2W_{15}\}$, under normal reaction conditions. This macrocation is found to decompose slowly in the presence of $\{P_2W_{15}\}$ and in doing so, helps to buffer the reaction medium leading to the formation of a nanosized tetrahedral polytungstate molecule $K_{21}Na_8[KFe_{12}(OH)_{18}(\alpha\text{-}1,2,3\text{-}P_2W_{15}O_{56})_4]\cdot 70H_2O$.[43] This 21 kDa POM cluster is found to be water-stable as was directly observed in solution/gas phase using electrospray mass spectrometry. In the crystal lattice, the tetrahedral anionic cluster units are inter-connected *via* external potassium ions to form an extended 3D network in the solid state with an accessible solvent volume of 6000 Å^3 per unit cell. This study was partly inspired by the works of Mizuno *et al.*, who have extensively used similar metal–organic macrocations for example: $[Cr_3O(OOCH)_6(H_2O)_3]^+$ with POM clusters resulting in interesting framework materials.[44]

Looking for new organic cations as shrink-wrapping agents, we used *N*,*N*′-bis(2-hydroxyethyl)piperazine (BHEP), which is found to act as a tri-functional species being a cation, ligand and buffer in POM synthesis. The ethanol arms attached to the nitrogen donors of the piperazine ring add flexibility to the ligand and form flexible coordination environment for the ligation of transition metals. BHEP can effectively buffer the pH range 4–8 allowing precise pH control. These properties make BHEP an interesting structure directing cation in POM synthesis. Two new POM

architectures, the dimeric cluster unit $[\{PMnW_{11}O_{39}\}_2(PO_4)]^{13-}$ and a 2D network-based on $[P_2Mn_4W_{18}O_{68}]^{10-}$ anions are isolated at pH 6.05 and 6.80 respectively using BHEP as buffer, encapsulating cation and ligand.[12] The dimeric cluster unit, formulated as $(H_2BHEP)_5(HBHEP)Na_2[(PMnW_{11}O_{39})_2\{PO_4\}]\cdot 18H_2O$ is composed of two α-$[PMnW_{11}O_{39}]^{5-}$ clusters connected by a bridging phosphate unit that links the Mn^{2+} centers attached to the mono-vacant Keggin entity. This moiety is stabilized, in the solid state, by the surrounding four H_2BHEP ions. The 2D network, $(H_2BHEP)_3Na_4[P_2Mn_4W_{18}O_{68}]\cdot 15H_2O$, is synthesized using a slight increase of pH and temperature in comparison to the dimeric compound. However, the structure of this new compound was entirely different; consisting of two $\{B\text{–}PW_9O_{34}\}$ units sandwiching four manganese centers between them in a belt like fashion. The synthesis of these compounds reiterates the multifunctionality of the BHEP ligand and the importance of solution pH in determining the nature of the resulting POM architectures under otherwise identical reaction conditions.

The important pH buffering capacity of BHEP is revealed in the synthesis of three Co(II)-containing silicotungstates *viz*. $[Co_3(H_2O)(B\text{-}\beta\text{-}SiW_9O_{34})(B\text{-}\beta\text{-}SiW_8O_{29}(OH)_2)]^{12-}$, $[Co_3(H_2O)(B\text{-}\alpha\text{-}SiW_9O_{34})(B\text{-}\beta\text{-}SiW_8O_{31})]^{14-}$, and $[Co_9Cl_2(OH)_3(H_2O)_9(B\text{-}\beta\text{-}SiW_8O_{31})_3]^{17-}$ which have been observed before only as dimeric or higher nuclearity cluster complexes. The synthetic strategy employed involves the reaction of Co(II) ions, the dilacunary $[\gamma\text{-}SiW_{10}O_{36}]^{8-}$ polyanion and the bulky organic cation BHEP in basic media at pH 8.0–9.0.[45] Although the BHEP ligand is not incorporated in these structures, the fact that these clusters do not form in the absence of BHEP in the reaction medium, led to the conclusion that this amine ligand plays a vital role in the isolation of these intermediate clusters, by acting as a buffer at these high pH values.

A prototype of a 3D polyoxometalate framework based on pure metal oxides and constructed without the use of external linkers to connect the polyanionic framework nodes has been achieved by the reaction of the divacant lacunary polyoxometalate $[\gamma\text{-}SiW_{10}O_{36}]^{8-}$ with Mn(II) in the presence of morpholinium cations and potassium permanganate, under strict pH control. This extended modular framework made up of POM building blocks incorporates "active sites" capable of responding to guest inclusion.[46] The resulting pure metal oxide framework, $[(C_4H_{10}NO)_{40}(W_{72}M_{12}O_{268}X_7)_n]$ ($M = Mn^{III}$, $X = Si$), based upon Mn-substituted Keggin-type POM building

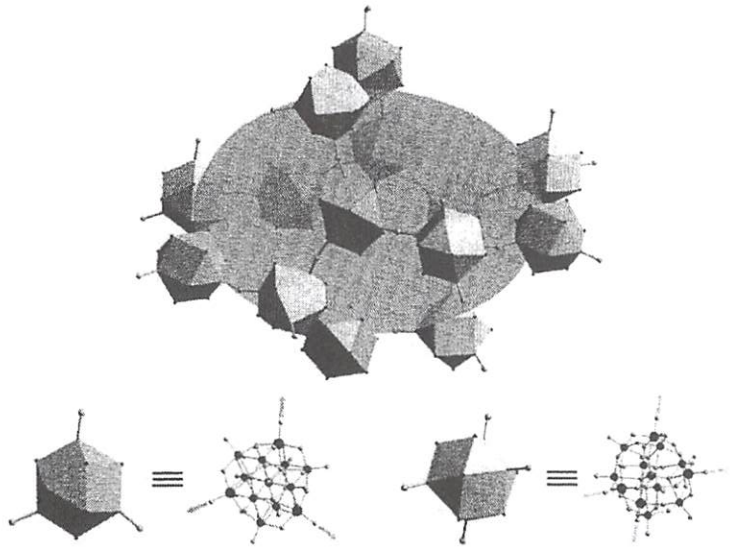

Fig. 13. Illustration of the nanosized pockets in $[(C_4H_{10}NO)_{40}(W_{72}Mn_{12}O_{268}Si_7)n]$ highlighted by the purple ellipsoid (dimensions: ~ 2.7\2.4\1.3 nm). The trigonal (rose) and tetrahedral (yellow) building block connectors are shown at the bottom; rose and yellow arrows highlight the connecting modes. **See Color Plate 10.**

blocks encloses elliptical pockets of 26.85\23.62\12.93 Å size and house solvent molecules and morpholinium cations in these pockets, Fig. 13. This material can undergo a reversible redox process that involves the simultaneous inclusion of the redox reagent with a concerted and spatially-ordered redox change of the framework. Importantly, this compound can be repeatedly disassembled and reassembled without any structural changes by dissolution in hot water followed by recrystallization. These unique properties define a new class of POM-based materials that bridge the gap between coordination compounds, metal–organic frameworks and solid-state oxides. Furthermore, it has been shown that all the Mn(III) centers in the oxidized form of this compound can be "switched" to Mn(II) using a suitable reducing agent to give the fully reduced framework. Moreover, the redox processes can be precisely followed by the single-crystal to single-crystal transformation between the oxidized and reduced states of the framework.

Extending the building block approach further by using very large building blocks such as a superlacunary $[H_7P_8W_{48}O_{184}]^{33-}$, $\{P_8W_{48}\}$, polyoxoanion and transition metal ions such as Co(II) as linkers, two cyclic cobalt-substituted heteropolyoxometalate frameworks $K_{15}Li_5[Co_{10}(H_2O)_{34}(P_8W_{48}O_{184})]\cdot 54H_2O$ and $K_8Li_{12}[Co_{10}(H_2O)_{44}(P_8W_{48}O_{184})]\cdot 60H_2O$ have been synthesized under strict control of pH and buffer. In both these frameworks, the central crown cavity of $\{P_8W_{48}\}$ is functionalized by a total of six Co(II) ions and additional Co(II) ions are grafted onto then outer rings extending the Co(II)-$\{P_8W_{48}\}$ anions into 1D chains in the former and to a 3D network in the latter.[47] As we have seen from the above examples, the combination of "building block approach" of POM synthesis with "shrink wrapping" cation technique has yielded several novel architectures and framework materials. It is to be noted here that, most of these materials are derived starting from simple POM building blocks such as lacunary Keggin or Dawson cluster derivatives. The most exciting aspect of this approach lies in the possibility of developing some true porous POM based materials starting from large, inherently porous POM clusters such as $\{P_8W_{48}\}$, $\{Mo_{154}\}$ etc. having open cavities at the center.[47]

2.3. *Organic-inorganic hybrids POMs*

An important step in POM chemistry towards functional materials is the development of organic–inorganic hybrid clusters by covalent functionalization which allows the synergistic combination of the properties of metal–oxo clusters and organic units, thereby allowing to fine tune the cluster properties such as solubility, redox properties, biological activities and so on.[24] Out of the various methods used for the covalent functionalization of POM clusters, grafting of tris(hydroxymethyl)aminomethane and its derivatives (denoted hereafter as TRIS) on to clusters is an important approach, as this group of molecules is geometrically well suited for grafting onto Anderson, Wells-Dawson and Lindqvist-type clusters.[48] Many POM hybrids containing TRIS as a linker between organic moieties and POM units are being developed for their potential applications as polymer support, POM based gels, and as light harvesting complexes.[49]

An interesting framework material, assembled purely through hydrogen bonding interactions, is achieved using an Anderson-based organic–inorganic hybrid cluster as the building block.[50] In the development of this framework material, a TRIS tethered pyrene moiety was covalently grafted onto a Mn-Anderson cluster, leading to the isolation of the hybrid cluster $TBA_3MnMo_6O_{18}\{(OCH_2)_3CNH–CH_2– C_{16}H_9\}_2\cdot 2DMF\cdot 3H_2O$ with properties different from that of pure building blocks. Furthermore, the self-assembly of this [Mn- Anderson(TRIS-pyrene)$_2$]$^{3-}$ building block together with TBA cations produces a nanoporous framework with nanoscale solvent accessible 1D channels in the solid state. This material appears to be stable until 240 °C despite being constructed from very weak C–H···O Mo hydrogen bonding interactions. The guest-uptake measurements revealed that the framework is nanoporous and is able to absorb up to 12% by weight of chlorobenzene.

Using TRIS-grafted Mn-Anderson clusters as the building block and Ag cations as linkers, the hybrid compounds $\{Ag_3[MnMo_6O_{18}\{(OCH_2)_3CNH_2\}_2(DMSO)_5]\cdot 3(DMSO)\}_n$; and $\{Ag_3[MnMo_6O_{18}\{(OCH_2)_3CNH_2\}_2(DMSO)_6(CH_3CN)_2]\cdot DMSO\}_n$ have been synthesized. These compounds having 1D chain structure form fibers on the Si surface >10 mm in length with a diameter of *ca.* 0.5 mm indicating that such hybrid clusters have potential for use in the self-assembly of functional materials.[51] Using long alkyl chain cations, the hydrophobicity of certain POM clusters could be increased, thus imparting new materials properties to such clusters. In an attempt to develop amphiphilic hybrids, we have successfully attached long (C-16 and C-18) alkyl chains onto TRIS grafted Mn-Anderson cluster by manipulating the reactivity of the free $–NH_2$ group of the TRIS moiety. Some of these long alkyl chain grafted hybrids indeed exhibited amphiphilicity forming supramolecular vesicles in solution.[52] Further, cations are exchanged from TBA to dimethyldioctadecyl ammonium (DMDOA), inducing new properties to these hybrids such as increased hydrophobicity. It is found that, some of these new materials form interesting microstructures on surfaces and exhibit interesting physical properties including phase transition and nanoparticle formation.[53]

Moving on to larger clusters, we have developed a series of TRIS grafted Dawson-like clusters to study their self-assembly in solid state and in solution. TRIS derivatives containing free $–NH_2$, $–NO_2$ and $–CH_3$ functionalities $H_2N–C(CH_2OH)_3$, $O_2N–C(CH_2OH)_3$ and $H_3C–C(CH_2OH)_3$ were successfully grafted onto the V_3 capped Dawson-like cluster $[P_2V_3W_{15}O_{62}]^{9-}$, resulting in a series of hybrid POM cluster anions having the general formula $[X\text{-}C(CH_2O)_3P_2V_3W_{15}O_{59}]^{6-}$, where X = $–NH_2$, $–NO_2$

or $-CH_3$. It is found that these hybrid clusters are capable of acting as supramolecular building blocks and are capable of self-assembling into larger supramolecular structures through hydrogen bonding interactions between the grafted TRIS moiety and the cluster oxygen atoms in solid state and in solution. Most importantly, it is found that the formation of these supramolecular architectures is controlled by the nature of the grafted H-bonding organic cap and/or the solvent system employed. Crucially, the NH_2-capped cluster anion $[H_2NC(CH_2O)_3P_2V_3W_{15}O_{59}]^{6-}$, on crystallization from acetonitrile, gave a fully H-bonded supramolecular assembly having a distorted tetrahedral structure, $(TBA)_{16}H_8[H_2NC(CH_2O)_3P_2V_3W_{15}O_{59}]_4 \cdot 8(CH_3CN)$; while crystallization from DMF led to $(TBA)_4H_2[H_2NC\text{-}(CH_2O)_3P_2V_3W_{15}O_{59}] \cdot 3DMF$ in which H-bonding between cluster and DMF molecules led to the formation of an infinite hydrogen-bonded chain structure in the solid state (see Fig. 14).

The role of the H-bonding ability of the organic caps of these cluster hybrids $[X\text{–}C(CH_2O)_3P_2V_3W_{15}O_{59}]^{6-}$, where X = $-NH_2$, $-NO_2$ or $-CH_3$ in forming multiple aggregates in solution and gas phase was analyzed by

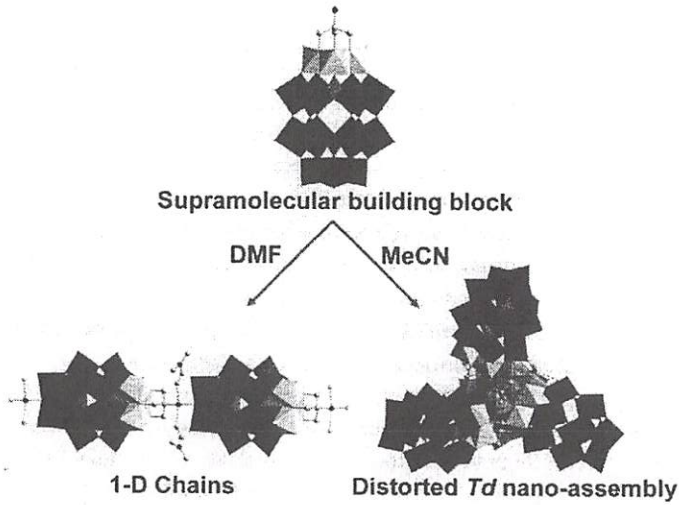

Fig. 14. Solvent dependent formation of different architectures from tris-grafted $\{P_2V_3W_{15}\}$ clusters.

comparing their cryospray mass spectra. The CSI-MS studies confirmed the formation of hydrogen-bonded nano-structures in the solution as well as revealed valuable information about the mechanism of this self-assembly process. For example, the formation of hydrogen bonded monomer, dimer, trimer and tetramers are detected in the solution and gas phase by CSI-MS studies in the case of $-NH_2$ and $-NO_2$ capped hybrid clusters; even higher aggregations such as pentamers and hexamers were detected in solution and gas phase in the case of $-NO_2$ capped cluster (see Fig. 15). The detection of these higher aggregates in solution and gas phase actually points to the formation of a number of virtual clusters in the solution before crystallization of a particular cluster out of the solution phase takes place. Therefore, this study revealed that the covalent grafting of H-bonding organic caps onto POM clusters can precisely control the supramolecular self-assembly of cluster species in the solid state and in solution and also shows the existence of cluster aggregates in solution other than the one that crystallized out ultimately.[54]

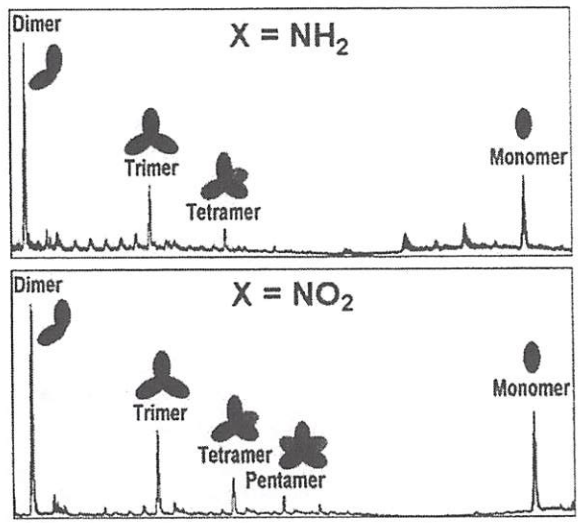

Fig. 15. CSI-MS spectra and supramolecular assemblies of $[X\text{–}C(CH_2O)_3P_2V_3W_{15}O_{59}]^{6-}$ clusters as a function of the different substituents (X) on the organic cap. Top X = $-NH_2$, bottom X = $-NO_2$.

In further extension of TRIS-Dawson hybrid cluster chemistry, we were successful in developing a class of POM-based "inorganic–organic–inorganic" hybrid clusters derived by grafting linear bis-(TRIS) ligands onto the V_3-capped Dawson-like cluster $[P_2V_3W_{15}O_{62}]^{9-}$. These inorganic–organic–inorganic "dumbbell" hybrids are approximately 3.4 nm long, representing the first examples of such dumbbells based on functional Dawson-like clusters.[55] Structural studies confirmed that these compounds contain two $\{P_2V_3W_{15}O_{62}\}$ cluster anions as dumbbell heads, which are linked together by linear bis(tris) ligands. The TBA cations are found to play a crucial role in controlling the self assembly of these clusters in the solid state. The TBA cations undergo extensive C–H···O hydrogen bonding interactions with the cluster heads of the dumbbells, effectively wrapping around them, hence making the dumbbell heads bulkier compared to their relatively thin middle part. This together with the peculiar zig-zag packing mode of these hybrids, lead to the formation of 1D channels along the crystallographic *b* axis in the crystal lattice. It is found that the diameter of these channels, ~1 nm, also corresponds to the length of the organic linker unit, thus suggesting a possibility of controlling the void space in similar hybrid dumbbell systems by changing the length of the linker unit (see Fig. 16). Furthermore, these hybrids are shown to self assemble in solutions forming vesicles as proved by light scattering and transmission electron microscopy (TEM) techniques.[55]

3. Extended Architectures Based on Transition Metal Salts/Oxides: Tubes, iChells and Blackberries

Given the comparatively large size of the poly-anionic POM clusters and high charge, ion exchange reactions can result in a variety of assembly processes whereby the POM clusters can form super-colloids, microtubular architectures, and cellular compartments (see Fig. 17).

3.1. *Tubular systems: Mechanism of formation*

The transformation of POM crystals into the tubular architectures occurs when a solution of a bulky cation on a sparsely soluble crystal allows it to

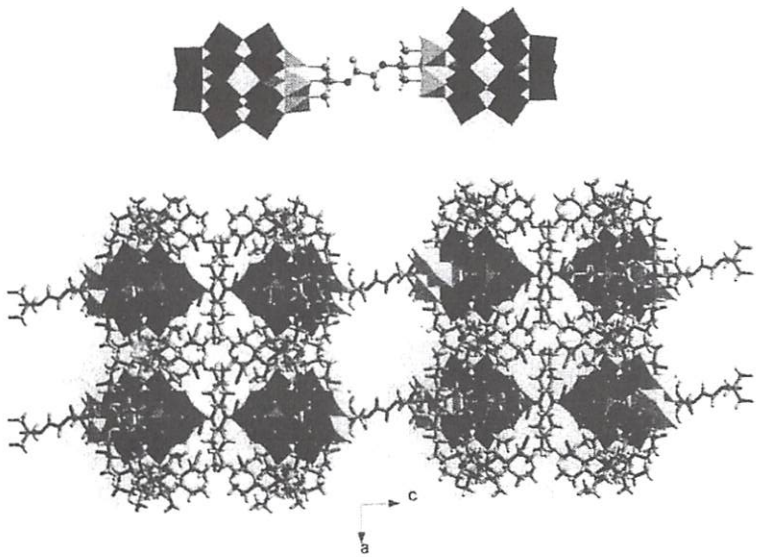

Fig. 16. Combined ball and stick and polyhedral representation of the "inorganic–organic–inorganic" hybrid cluster anion derived by grafting linear bis-(tris) ligands onto the V_3-capped Wells-Dawson-type cluster $TBA_5H_4[P_2V_3W_{15}O_{62}]$ (above) and the packing diagram (below) of the same compound showing the selective gathering of TBA cations around dumb-bell heads leading to voids in the crystal lattice. C (grey), H (white), N (blue), O (rose), W (violet polyhedra), V (yellow polyhedra), P (pink polyhedra). See **Color Plate 11**.

dissolve locally, and produce a hollow membrane mediated by the electrostatically driven aggregation of the POM-crystal and the bulky cation added to the solution which produces an insoluble matrix.[56] Once formed, the permeability of this membrane allows water to pass through and the osmotic pressure inside increases. When the system reaches a critical pressure, the membrane ruptures and the dissolved POM material that is contained within the membrane is ejected through the aperture, whereupon it comes into contact with the cation solution, leading to further aggregation (see Fig. 18). The aggregate is composed of the cations and POM anions bound electrostatically in a charge-balancing ratio.[57] Since water ingress at the crystal maintains a constant outflow of material through the opening, closure of the structure is not possible, and the

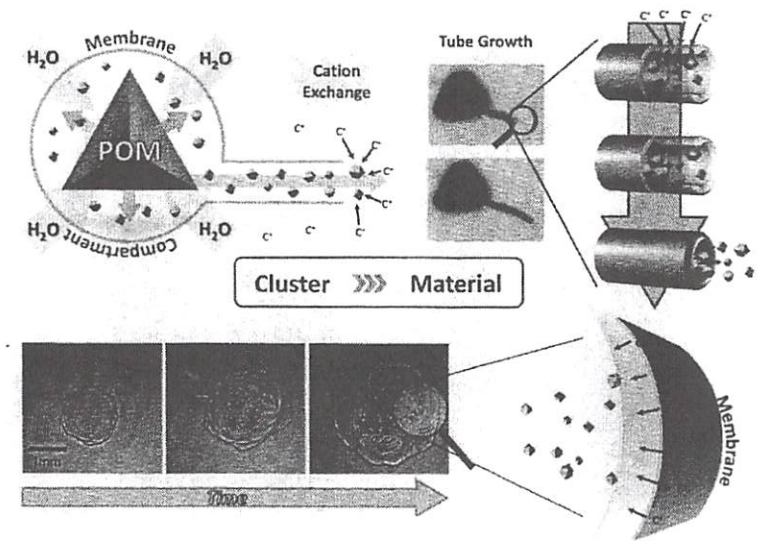

Fig. 17. Representation of how POM clusters can aggregate and form nano/micro-sized materials such as tubes and membranes.

aggregation produces extended tubular architectures. This process is able to transform a large number of crystals simultaneously (Fig. 19), and works for a wide range of POM including the so-called "Keggin Network" species (KN thereafter).[46] These polyoxometalate tubular architectures are always hollow and can be fabricated using a wide variety of clusters including catalytically active components and mixed tubes (fabricated from two or more POMs can also be made).

The flow of the POM-based solution is sustained while crystalline material is still present in the parent membrane, and continues to be dissolved. Consequently, the osmotic engine still pumps water and the system is kept in flux, resulting in continued tube growth until the material housed within the crystal is completely expended. If, for any reason, the flux is weakened or stopped, the tube growth stops immediately. The process of growth could theoretically allow a single tube to propagate until the crystal is entirely consumed, since the flow depletes POM

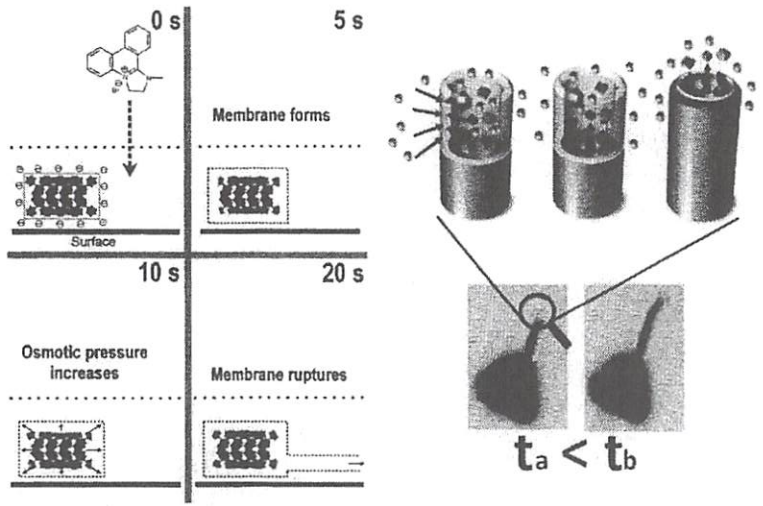

Fig. 18. Schematic representations of the mechanism involved in micro-sized tubular formations based on POM and organic cations. The resulting architecture is amorphous and can extend as far as 2×10^{-5} times the crystal size.

concentration in its neighborhood. This is, however, not the case and the growth often stops within 2–3 minutes (although growth can persist for as long as 30 minutes). This may be due to the pressure in the tube causing a new rupture point, either at the source or somewhere along the tube, in which case, tube growth continues from that new rupture point and the original tube ceases to grow. The likelihood of this occurrence is increased when the growing end of the tube encounters an obstruction on the surface. The diameter of a growing tube can be controlled by changing the concentration of cations, and has been demonstrated in the range of low concentrations for the cation methyl dihydroimidazophenanthridinium, DIP-Me.[59] Increasing the cation concentration leads to a decrease of the tube diameter, whereas addition of pure water (to decrease the overall cation concentration) leads to an increase of the tube diameter.[60] In the limiting case, when the cation concentration is raised too far, tube growth will not propagate/initiate because any rupture in the membrane will be immediately sealed.

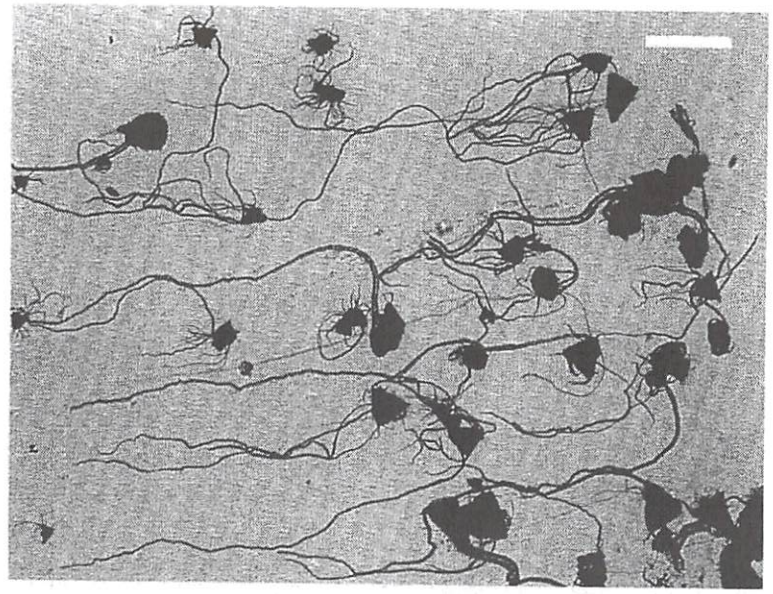

Fig. 19. Picture of a large number of crystals that have all been transformed from crystalline form to crystals that have sprouted very long tubes on addition of large cations to the aqueous solution in which the tubes are immersed. The photograph was taken 15 mins after cation addition. Tubes have grown in a uniform direction due to a bulk flow of solvent in this system (from right to left). The white scale bar is 500 μm long.

These changes can be made in "real-time", while the tube is still growing, and repeated many times to predictably produce a tube with variable diameter. Once the initial membrane has formed around the crystal and tube growth has started, the limiting rate at which water can cross membrane, and therefore the rate of POM dissolution, becomes fixed and is related directly to the surface area of the membrane. Since the membrane forms on the surface of the crystal, the initial crystal size can be used to estimate the membrane surface area and correct for this effect. The growth rate then varies proportionally with cation concentration over the range where tube growth can occur (see Fig. 20). The control of diameter by changing cation concentration can be explained in terms of the availability

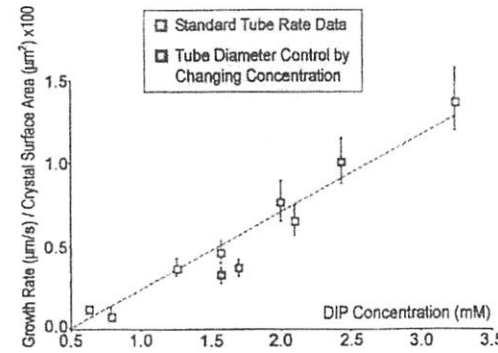

Cation conc. (mM)	Speed/Surface μm/s/μm² x100
0.4	0.002
0.6	0.012
0.8	0.007
1.3	0.037
1.6	0.046
2.1	0.065
3.3	0.138

Fig. 20. Plot of growth rate/crystal surface area against the overall concentration of DIP, showing how the diameter is related to the cation concentration. Red squares show the linear decrease in growth rate as the concentration is decreased, and blue squares show rate data for a tube in which the concentration of DIP-Me is varied while it is growing. Note: The crystal surface area is considered as it relates directly to the limiting rate at which water can enter the membrane surrounding the crystal, and therefore the rate of POM dissolution and tube growth. This allows direct comparison of tubes grown from crystals of varying sizes and shapes. **See Color Plate 12.**

of cations to reach a critical level of aggregation required for precipitation of the tube forming material. The increase of the cation concentration in the neighborhood of a growing tube supplies a greater density of cations and so fragments in the plume of ejected POM material will travel less distance before they encounter sufficient cations to aggregate. Once the solid material is aggregated and joined as part of the tube wall, it is relatively inflexible, and so the diameter of the tube decreases. In the reverse scenario, when the cation concentration is reduced, the ejected plume of POM material expands further before the critical aggregation point is reached and so the tube diameter increases. If the concentration of cations is reduced too far, aggregation may occur too far away for fragments to join the walls and the tube may cease to grow.

The mechanism of tube growth is osmotically driven and this is clearly seen by the effect of changing the solution ionic strength.[57] When 2–3 drops of a saturated sodium chloride solution in water is added to a system

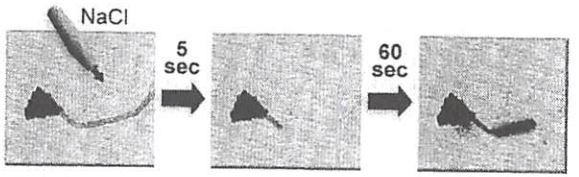

Fig. 21. Addition of aqueous sodium chloride solution to a growing tube (Keggin Network crystals—KN—/ DIP-Me) causes tube growth to temporarily stop as a competitive osmotic flow is initiated. After equilibration of the sodium chloride concentration across the membrane (30–60 s), tube growth continues, not necessarily on the same path.

where tube growth has already initiated, the growth process is temporarily halted (Fig. 21). On addition of the brine outside, ionic strength of the solution is increased to around 13 × the original number and so the osmotic potential across the membrane is reversed, since the region of lowest ionic strength is now the inside of the membrane surrounding the POM crystal. The salt injection causes a second, competitive, osmotic pump to initiate, drawing solution into the membrane surrounding the crystal, through the tubes. This disrupts the osmotic growth mechanism, as no POM material can be ejected against this new flow direction. Competition between the newly added ionic species and the aggregated material in the tube walls leads to local formation of $POM{\cdot}Na^{+}_{x}$ and $DIP{\cdot}Cl^{-}_{x}$ species, which causes some dissolution of the tube walls.

Once the concentration of NaCl inside the membrane and tube has been equilibrated with the surrounding solution the original osmotic pump, whereby dissolved POM material is ejected through the tube, becomes predominant once again. The continued presence of NaCl in the solution no longer influences the osmotic potential directly. However, it does change the solubility properties of the components and the aggregate, leading to significantly thicker/less consolidated tube walls. Without further perturbation, the system will once again continue the morphogenesis until all the crystalline material is expended. The reaction to salt addition, and the recovery of tube growth, demonstrates that the growth process can be considered follow a "siphon" like mechanism, in that the concentration of dissolved POM material is maintained along the whole length of the tube. While the POM material remains available in crystalline form, the

local concentration of POM material in solution will tend towards saturation, because of the low solubility of the POM. Once a membrane rupture has occurred, and tube growth is under way, the ingress of water into the membrane is controlled by the removal of saturated solution from the membrane "chamber" through the tube. This means that the POM material is at saturation along the length of the tube, and as a consequence of this, the rate of tube growth remains constant, even as the tube extends several hundred microns from the parent crystal.

The overall solubility of the crystals is critical in tube growth initiation. When the pH of the overall solution is raised after tube growth initiation, thus modulating the solubility of the POM, the rate of tube growth increases as expected. However, if the pH is raised before tube growth has started, only precipitation is observed, as the crystal dissolves too rapidly for the initial membrane-shell to become consolidated.[60] The key properties of the POM material that influence the growth of tubes are the size and solubility of the crystal. These govern both the amount of material that can be dissolved from the crystal surface and the rate at which it can aggregate. The size and shape also directly influence the surface area of the membrane which later controls the rate at which water can enter and therefore the rate of tube propagation. Temperature and pH can be considered as "secondary factors" as they also affect a growth process but do so by modulating the crystal solubility.

It is important to consider the initial stages of tube growth, as this is the critical time where the membrane shell is formed. If the membrane is weak or the dissolution of the crystal is too rapid, there will not be sufficient containment to produce the required osmotic potential for tube growth. Conversely, tube growth will also not initiate if the aggregated membrane is too strong to be broken by the osmotic pressure within, or if the cation concentration is so high that ruptures are instantly "self-healed". The properties of the cation must also be considered. In experiments with larger volumes (> 1 ml) the solution concentration can be considered as a constant throughout the tube growth. Indeed, even if the tube formation depletes the cations in the medium immediately surrounding the growing end of the tube, the point of growth continuously moves forward into areas where the cations are still present. In experiments conducted in droplets, the concentration change

over time becomes more significant and indeed tube diameter is seen to increase slightly. When a droplet experiment is continuously supplied with fresh cation solution, so as to truly maintain a constant concentration, no change in tube diameter is observed. However, it is important that the charge and size of both the cations and anions are considered, as the aggregation process is electrostatically controlled. This is because we have established that the aggregation of POM and cation occurs in a ratio that is expected to result in full charge balancing,[56] and it can be tentatively proposed that this modulates both the porosity of the initial membrane and the thickness of tube walls. It is also observed that with the same POM, the use of more highly charged cations gives rise to faster growing, narrower tubes since a lower local cation concentration is required in order to cause aggregation.

3.2. *Particular tubes/minimal systems*

In this section, we focus on the control parameters that can be made to a growing tube. The seeds and more importantly tube from needles will be discussed. Initiation of tube growth requires a sufficient local concentration of cations to be present in order to form the membrane around the POM crystal and it is therefore not possible to grow tubes under normal conditions in pure water or solutions with very low cation concentration. However, since the process only requires a local availability of cations, it is possible to construct a minimal system, where the cations are coated onto the crystal of the POM and are in sufficient concentration to produce tubes. This localization is achieved by depositing a shell of cation material all around the POM crystal using a cation solution in a solvent in which the POM is totally insoluble. The introduction of such a micro sized core-shell particle into pure water gives rise to a situation where initial membrane formation is instantaneous, and the remaining cations diffuse around the neighborhood of the crystal. This 'seed' then proceeds to grow tubes by the normal mechanism (Fig. 22), although due to the limiting availability of cations, the membrane around the parent crystal is weak and so several rupture points occur, leading to multiple tubes. The tubes grow rapidly and, as expected, their diameters increase due to the decreasing concentration of cations as the growing end travels further from the source of cations (precisely the same effect as lowering the cation concentration to control the diameter in

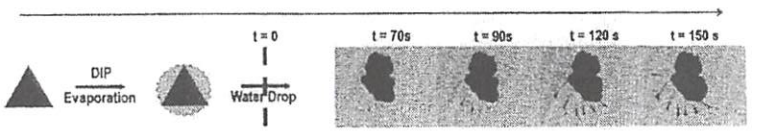

Fig. 22. Description of the "seed" experiment. A crystal of Keggin Net is coated by organic molecules (DIP in this case) through multiples evaporation of a methanolic solution containing the cation. Crystals of this particular POM has proven to be nearly insoluble in such media and end up coated with several layers of DIP. Upon pure water immersion, such a solid releases slowly its organic molecules before starting to dissolve, with the outcome of a micro-sized tube formation. However, in this experiment the amount of organic material is clearly limited and therefore the tubes become bigger and bigger until they stop to grow due to the rarefaction of the DIP molecules.

previous experiments). Growth continues until the tubes reach a region where there is insufficient cation concentration, after which they remain open and dissolved POM material is continuously expelled until the crystal is expended. Because the tubes remain open and material is pumped out through them, the osmotic pressure is continuously relieved and further ruptures to the membrane around the parent POM crystal do not occur.[57]

To explore different avenues for the fabrication of the tubular architectures it was postulated that growth of such tubes could be possible from a narrow aperture involving an extrusion process. To investigate this, crystals of KN compound were dissolved in water and the filtered solution was injected into a cation solution (DIP-Me) *via* a 5 micron aperture needle, using a syringe pump. As predicated, it was possible to fabricate 25 micron diameter tubes up to 500 microns in length. Fabrication was possible both *via* extrusion when the needle was both stationary and moving, demonstrating that such tube 'drawing' could be used to make pre-designed patterns with tubes (Fig. 23). However, the main limitation is once again the solubility, and 'writable' tubes require relatively insoluble POM-based materials; injection of the more soluble POMs did not result in the formation of tubes.[57]

3.3. *Growth control*

The overall solubility of the crystals is critical not only in modulating the rate of tube growth, but also in tube growth initiation. When the pH of the overall solution is raised after tube growth initiation, thus

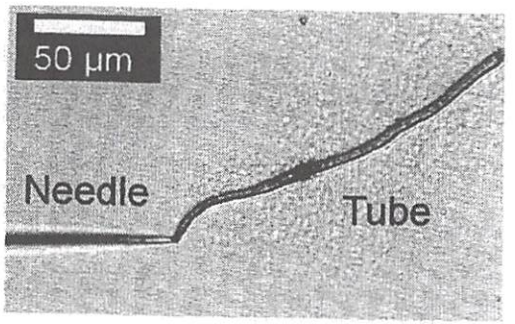

Fig. 23. Description of the "tube from a needle" experiment. Crystals of the Keggin Net specie are dissolved into water to a known concentration before being injected into a solution containing some DIP cations. It is possible to "draw" a particular shape with the tube formed.

modulating the solubility of the POM, the rate of tube growth increases as expected. However, if the pH is raised before tube growth has started, only precipitation is observed, as the crystal dissolves too rapidly for the initial membrane-shell to become consolidated.[59] The key properties of the POM material that influence the growth of tubes are the size and solubility of the crystal. These govern both the amount of material that can be dissolved from the crystal surface and the rate at which it can aggregate. The size and shape also directly influence the surface area of the membrane which later controls the rate at which water can enter and therefore the rate of tube propagation. Temperature and pH can be considered as "secondary factors" as they also affect a growth process but do so by modulating the crystal solubility. It is important to consider the initial stages of tube growth, as this is the critical time where the membrane shell is formed. If the membrane is weak or the dissolution of the crystal is too rapid, there will not be sufficient containment to produce the required osmotic potential for tube growth. Conversely, tube growth will also not initiate if the aggregated membrane is too strong to be broken by the osmotic pressure within, or if the cation concentration is so high that ruptures are instantly "self-healed".

In addition, the overall diameter and growth rate of the tube are not altered by the changes in direction and this is consistent with a growth mechanism where the rate of growth is determined by the surface area of the parent crystal and the concentration of available cations. In order to

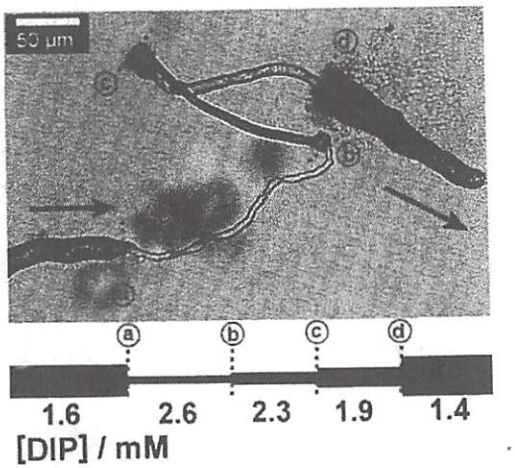

Fig. 24. Size control of a growing tube by altering the available concentration of cations at points (a), (b), (c), and (d). The estimated concentrations at each point are shown in the lower section.

demonstrate this, and to show that the tube diameter can also be controlled, the overall concentration of DIP-Me was altered while the tube was growing. Increasing the concentration of DIP-Me caused the tube to become much narrower and to grow faster while addition of water, thus decreasing the overall concentration of DIP-Me, caused the tube to become much wider and to grow more slowly (Fig. 24).[59]

To achieve direction control, a potential difference of 9 V was applied across opposite pairs of electrodes resulting in localized heating and thus, bulk flow of the solvent through convection. Growing microtubes were observed to always alter their direction of growth so as to grow towards the cathode. The most accurate control was achieved when the tube growth was in the area equidistant between the electrodes and so direction control experiments were exclusively carried out in this area. Application of the potential also caused aggregation of organic material at the anode but ^{1}H-NMR studies of the starting material, and aggregated precipitate, show that the organic framework remains unaltered. However, there is a reduction in the lifetime of tube growth and this due to migration of the charged species towards the electrodes and consequent reduction

of concentration in the area in which direction control experiments are carried out.[59] By carefully controlling the direction of the applied electric field and the duration for which it was applied, several different motifs were generated in the growing tube and these fall into two categories. In the first, and most simple example, the growth is continuously switched between two directions which opposite to one another, creating a tight wave-like shape with 180° bends (Fig. 25(a) — top right). In the second, more advanced category, both sets of perpendicular electrodes are used either to create a zig-zag pattern with 90° bends (Fig. 25(b)) by switching between two directions or more complex motifs of 90° bends, for which the tube is steered in all four directions (Figs. 25(c,d)).[59]

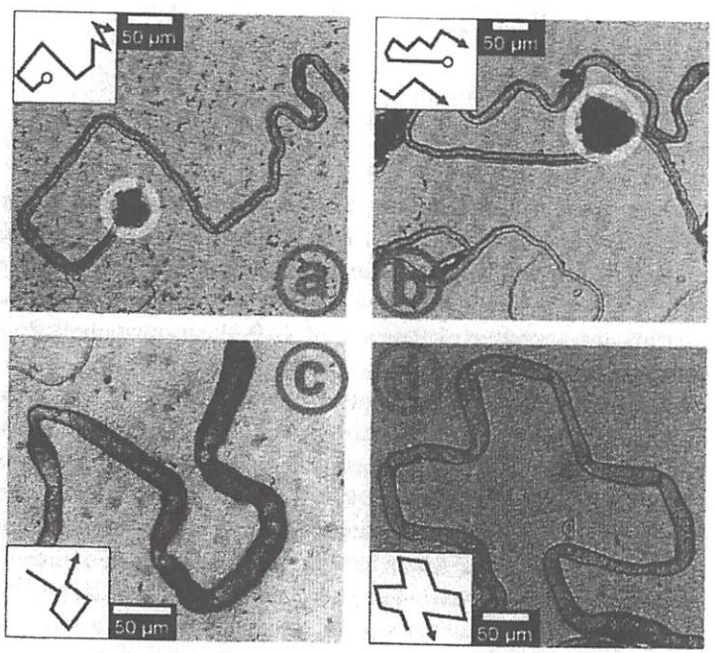

Fig. 25. Motifs "drawn" by controlling the tube growth direction. (a) 90° bends followed by a series of 180° turns. (b) A series of 90° bends to make a zig-zag motif. (c) 90° bends to form a square. (d) A series of 90° turns making a cross shape. Circles indicate the crystals from which tubes are growing. Inset diagrams show the direction of the tube growth.

It will be interesting to see how this discovery is applied since it is now possible, at least in principle to direct the assembly of nano-molecular POM clusters to form micro-tubular architectures with a configurable composition, diameter, and orientation/shape. The ability to use intrinsically catalytically active POMs in the fabrication of the tube walls raises the real possibility of using this discover to develop a new range of micro-devices.

3.4. *Formation of inorganic-chemical cells: iCHELLs*

The formation of membrane material can be achieved *via* an 'extrusion-exchange' mechanism whereby the injection of a solution containing large POM anions along with small cations into a solution containing the organic cations accompanied by small anions.[60] This leads to an ion exchange reaction at the solution interface initiating the fabrication of an insoluble aggregate of the two large species at the boundary (see Fig. 26).

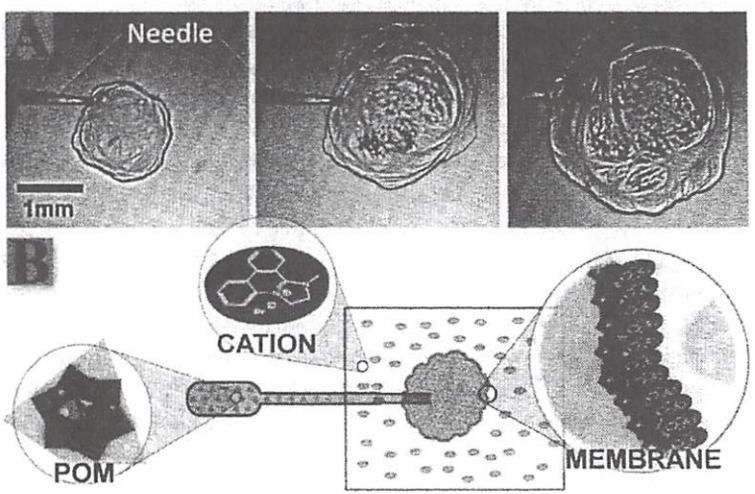

Fig. 26. (a) A sequence of images showing the formation of a 1.2 mm diameter cell as the POM solution (phosphotungstic acid) is injected into the solution of the organic cation (methyl dihydroimidazophenanthridinium, DIP-Me). Needle aperture: ca. 20 μm. (b) Schematic illustration of the "extrusion-exchange" mechanism of membrane formation. One component is injected into a solution of the other, in which cation exchange occurs on the POM, hence leading to aggregation.

This insoluble aggregate differs significantly from simple precipitation due to the morphological persistency of the resulting structure, which shows no permeability to the component species on either side of the membrane, effectively separating the initial solutions. In the general case, while observing the system through an optical microscope, an aqueous solution of the POM, phosphotungstic acid, is injected into a droplet of aqueous cation (in this case a heterocyclic-based phenanthridinum, cation)[58] using a micromanipulator needle resulting in the immediate formation of a membrane which partitions the two solutions. The reverse scenario, in which the cation is injected into the POM solution, also causes membrane formation. The membranes so far produced have been shown to be flexible, encompassing sack-like architectures with controllable diameters that span 50 μm up to several millimeters. These structures can be deflated and re-inflated several times by drawing the contents back into the micromanipulator and then re-injecting. Several such architectures can coexist with one another, allowing bulk manufacture of sack structures, and show no tendency to coalesce upon contact, instead remaining distinct entities. During the fabrication process, or when deliberately damaged, any rupture in the membrane surface is immediately repaired as the two components come into contact with one another.

Membranes can be produced using a range of organic cations (e.g. from heterocylic derivatives of phenanthridiniums (DIPs) to the highly fluorescent $Ru^{II}(bipy)_3(BF_4)_2$ (bipy = 2,2'-bipyridyl)) and a range of POMs such as $\{PW_{12}\}$ and phosphomolybdic acid ($H_3PMo_{12}O_{40}$, $\{PMo_{12}\}$) through to more complex materials including the very large 3.6 nm wheel-shaped $\{Mo_{154}\}$ cluster.[61] This self-assembling system is not, however, confined to the use of polyoxoanions from dissolved crystals as formation of membranous material was also observed upon injection of a simple phenanthridinum-cation, and sodium phosphate (dibasic, Na_2HPO_4), into an aqueous solution of sodium tungstate (Na_2WO_4). Membranes do not form in a similar experiment in the absence of phosphate anions, suggesting that the formation of a structured anion (i.e. a Keggin polyoxometalate POM which can only be templated from phosphate) is required to form the bulk membrane. The phenomenon is also not limited to purely aqueous media, as membranous sack structures can be produced in up to 1:1 water/acetonitrile mixtures and also in aqueous ethanol solutions. This

property increases the versatility of the resulting membranes as it allows them to be used to encapsulate organic species which are insoluble in pure water.

The structure of the membranes produced using this modular "extrusion-exchange" process can be studied using scanning electron microscopy of dried samples, and shows that variation of the POM starting material results in large differences in the morphology of the resultant material. Small POM anions, with a low charge of –3, such as the 1.2 nm $\{PW_{12}\}$ produces thinner (1–2 μm), more wrinkled, membrane surfaces, while higher 1.8 nm sized $\{W_{48}\}$ POM clusters, with an overall charge of –40, give a much thicker, more featureless membrane geography. Cracks formed in the membranes, during the drying process in preparation for SEM analysis, show that these membranes can be up to 5 μm in thickness. Closer analysis of the surfaces of both types of membranes reveals similar structures of continuous raised areas in the region of 50–100 nm in width. These raised areas are most pronounced in rough, broken areas of the surface where deep valleys in the material can be observed. We propose that the membrane is composed of discrete nanoparticles which are charge-balanced aggregates of the starting components, where the particle size is controlled by the POM cluster size and charge. Membranes produced from larger, more highly charged clusters are therefore likely to be thicker. Elemental analysis (for C, H and N) of the membranes shows that the composition of the individual components is retained and that the cations and anions aggregate in the correct ratio to exactly balance the overall charge, and this analysis is confirmed by EDX (Energy-dispersive X-ray spectroscopy) analysis. In the specific case of $\{PW_{12}\}$ or $\{PMo_{12}\}$ with the phenanthridinum based-cation DIP-Me, this gives a POM: Cation ratio of 1 : 3, while with the large and highly charged $\{Mo_{154}\}$ cluster, a ratio of 1 : 56 is observed.

The mechanical strength of $\{PW_{12}\}$-based membranes can be investigated using an AFM cantilever to tear the membrane and observing the deflection of the tip as tearing occurs. Initial results indicate that a force of ~110 μN is exerted before the tip tears the membrane when it is derived from simple DIP cations. This is around 100x less than the force required to rupture a biological vesicle wall. The strength of membranes can be enhanced by ~15% by using a larger, more highly charged dimeric DIP

cation in place of DIP-Me, probably due to the enhanced cross-linking ability of the cation. This demonstrates a method of controlling mechanical strength of these materials which will be extremely useful when designing and building membrane-based devices.

3.5. *iCHELL chemistry*

Since selective permeability is an essential feature in synthetic hybrid membranes, the materials can be tested by subjecting $\{PW_{12}\}$ containing sacks (in DIP-Me solution) to a flow of ammonium hydroxide solution and solutions of tetraalkylammonium hydroxides of varying chain lengths. Upon contact with any of these ammonium species, $\{PW_{12}\}$ immediately precipitates so it is easy to observe the time taken between addition of the ammonium salt outside of the sack and the precipitation of $\{PW_{12}\}$ inside. Treatment with ammonium hydroxide and tetramethylammonium hydroxide resulted in very rapid precipitation inside the sack. However, when larger tetraethyl- or tetrapropylammonium hydroxide was used, a significant lag before precipitation was observed and when tetrabutylammonium was added, no precipitation was observed, thus demonstrating that the membranes are more permeable to smaller molecules. Injection of either component into the other produces a membranous pouch, the construction of a sack within another sack is possible. These "nested" systems can be used to compartmentalize chemical reactions. As a simple demonstration of this, DIP-Me solution can be injected into a solution of $\{PMo_{12}\}$ and the resulting membrane sack was then further injected with a solution containing $\{PW_{12}\}$ with a small amount of potassium permanganate added, thus producing a smaller sack inside the first. Both remained stable for a period of several hours without merging or leakage, unless physically pushed together. Addition of hydrogen peroxide to the outer $\{PMo_{12}\}$ solution caused discoloration of the potassium permanganate after a short diffusion time, showing that the 'nested' system can be used to compartmentalize chemical reactions since the H_2O_2 is able to pass over both membranes and through the DIP solution. Compartmentalized sack to sack reaction systems would also be possible, where a sacks containing different reagents (able to cross the membrane at different rates) are brought into close proximity with one another, allowing sequences of chemical transformations to occur (see Fig. 27).

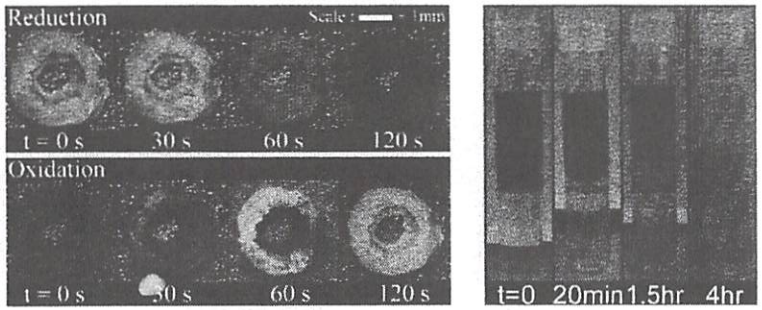

Fig. 27 (a) A schematic representation of one cell being grown inside another. A salt containing a large organocation (green) is injected into a salt solution containing a large POM anion (blue) forming a membrane. A second POM that contains another POM reagent (red) is injected into the first cell, producing a second membrane. Adding an external reagent (yellow) can then cause a reaction in the inner cell after a diffusion time. (b) Time-lapse images are shown below with the growth of a DIP-Me cell in $\{PMo_{12}\}$, followed by the construction of a $\{PW_{12}\}$ cell inside the encapsulated DIP-Me droplet. The $\{PW_{12}\}$ cell contains potassium permanganate and when hydrogen peroxide solution is added to the outer $\{PMo_{12}\}$ solution, discoloration of the $\{PW_{12}\}$ cell is observed after a few minutes. **See Color Plate 12.**

One of the major advances represented by the development of these membrane systems is to enable incorporation of chemically active components into the material. In the simplest case, the POM component of the membrane material represents a redox active species capable of being reduced to form blue reduced POM species by the action of a suitable reducing agent. After the addition of sodium dithionite ($Na_2S_2O_4$) to a solution containing a $\{PW_{12}\}$-DIP-Me membrane, the membrane quickly switches to the reduced blue form (Fig. 28 (a)). Subsequent washing of this blue material followed by addition of an oxidizing agent (e.g. hydrogen peroxide) led to the rapid loss of the blue color as the membrane was re-oxidized. This process proved to be reversible and could be repeated up to three times before degradation of the membranes. As well as forming closed, sack-like, architectures, membrane formation will occur at any interface between solutions of suitable cations and anions, allowing the formation of layered domains which are effectively phase separated by the intervening POM-DIP-Me membrane. We demonstrate this by forming a membrane across a glass vial, where the pH sensitive indicator,

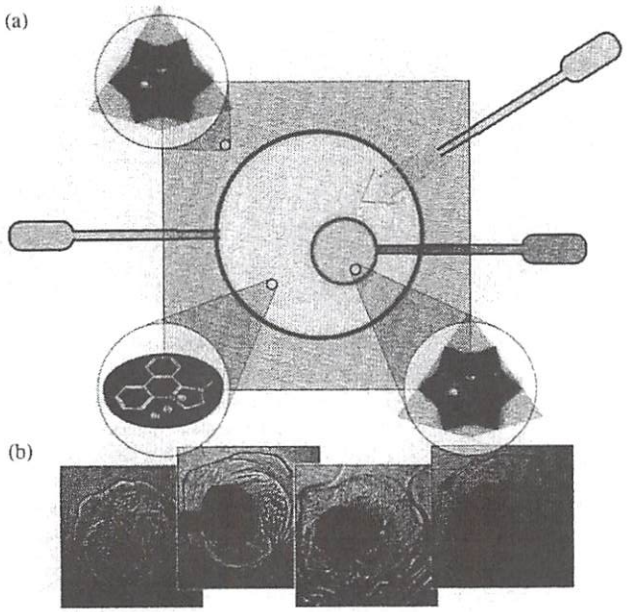

Fig. 28. (a) Addition of dilute sodium dithionite (reducing agent) to a washed membrane in water, results in the reduction of the POM over 120 seconds. After washing with deionized water, addition of hydrogen peroxide solution (30% v/v) to the same system causes the POM to become reoxidized over approximately 120 seconds. This process is fully reversible and can be repeated up to three times without significant membrane degradation. (b) Diffusion of H_3O^+ cations through a $\{PW_{12}\}$-DIP-Me membrane showing the change in color of the bromocresol purple in the upper DIP fraction from purple to yellow indicating the lowering of the pH in this region. **See Color Plate 13.**

bromocresol purple, which appears purple above pH 6.8, but yellow below pH 5.2, is encapsulated in the DIP-Me solution and separated from the inherently acidic POM $\{PW_{12}\}$. A color change from purple to yellow is observed in the cation solution over ~4 h, as the H_3O^+ cations diffuse through the membrane (Fig. 28 (b)).

Once formed, the membrane sacks can be successfully transferred out of their mother liquor, as long as they remain in a sufficiently high ionic strength environment. They are not stable if transferred into pure water, were osmotic pressure causes rapid expansion and rupture of the sack. The

supporting of membranes on polymer supports allows a number of further applications to be investigated, as the membrane coated matrix can be easily removed from the initial solution and washed several times without losing their structural integrity. We showed that our membranes can be grown on a supporting hydrogel matrix by sorbing the cationic membrane forming component into an anionic hydrogel material, such as partially deprotonated polyacrylic acid. The cation soaked hydrogel material was then immersed in a solution containing the POM component, forming membranous material on the surface of the hydrogel.

4. Conclusions

There is no doubt that POMs are extremely diverse, but in this chapter we have attempted to explore the unique nature of their high charge and large size. As large anions they are perhaps unique in chemistry, and therefore it is not surprising that POM-based molecules and materials are still throwing up many discoveries of new phenomenon. The other important aspect is the fact that POM structures mostly represent kinetically trapped units, and as such their reactivity can be controlled by successive ion exchange reactions. This is a rather simple yet profound realization since armed with this knowledge it is possible to develop routes to assemble functional materials and devices. The next challenge will be to harness these properties to develop a new generation of functional nano molecular and macromolecular systems.

Acknowledgements

The authors wish to acknowledge the University of Glasgow, WestCHEM and the EPSRC for funding. L.C. thanks the Royal Society/Wolfson Foundation for a merit award and would also like to acknowledge the many diverse and exciting collaborators beyond Glasgow that have contributed to the work discussed in this chapter.

References

1. (a) Pope M. T. and Müller A., *Angew Chem Int Ed Engl* **30** (1991) 34; (b) *Polyoxometalate Chemistry: From Topology* via *Self-Assembly to Applications*,

ed. Pope, M. T. and Müller, A. (Eds.) Kluwer, Dordrecht, 2001; (c) C. L. Hill (Ed.), Special issue on polyoxometalates, *Chem Rev* **98** (1998) 1–387.
2. Long D.-L., Tsunashima R. and Cronin L., *Angew Chem Int Ed* **49** (2010) 1736.
3. (a) Hasenknopf B., *Front Biosci* **10** (2005) 275; (b) Yamase T., *et al.*, *Inorg Chem* **45** (2006) 7698; (c) Kortz U., *et al.*, *Coord Chem Rev* **253** (2009) 2315; (d) Neumann R. and Dahan M., *Nature* **388** (1997) 353; (e) Rhule J. T., *et al.*, *J Am Chem Soc* **123** (2001) 12101; (f) Mishra P. P., Pigga J. and Liu T., *J Am Chem Soc* **130** (2008) 1548; (g) Noro S.-i., *et al.*, *Angew Chem Int Ed* **48** (2009) 8703; (h) Imai H., *et al.*, *J Am Chem Soc* **131** (2009) 13578; (i) Streb C., *et al.*, *Angew Chem Int Ed* **48** (2009) 6490; (j) Fleming C., *et al.*, *Nat Nanotechnol* **3** (2008) 229; (k) Mitchell S. G., *et al.*, *Chem Commun* (2009) 2712.
4. (a) Long D.-L., Burkholder E. and Cronin L., *Chem Soc Rev* **36** (2007) 105; (b) Long D.-L. and Cronin L., *Chem–Eur J* **12** (2006) 3698; (c) Kögerler P. and Cronin L., *Angew Chem Int Ed* **44** (2005) 844.
5. (a) Müller A., Kögerler P. and Kuhlmann C., *Chem Commun* (1999) 1347; (b) Cronin L., Kögerler P. and Müller A., *J Solid State Chem* **152** (2000) 57; (c) Cronin L., *et al.*, *Angew Chem Int Ed* **41** (2002) 2805–2808.
6. Müller A. and Roy S., *Coord Chem Rev* **245** (2003) 153.
7. (a) Contant R., *Inorg Synth* **27** (1990) 109; (b) Contant R. and Ciabrini J.-P., *J Chem Res Synop* (1977) 222; (c) Knoth W. H. and Harlow R. L., *J Am Chem Soc* **103** (1981) 1865; (d) Canny J., Tézé A., Thouvenot R. and Hervé G., *Inorg Chem* **25** (1986) 2114; (e) Kirby J. F. and Baker L. C. W., *Inorg Chem* **37**, (1998) 5537.
8. (a) Desiraju G. R., *Crystal Engineering: The Design of Organic Solids*, Elsevier, Amsterdam, (1989); (b) Braga D., Grepioni F. and Orpen A. G., ed., *Crystal Engineering: from Molecules and Crystals to Materials*, Kluwer Academic Publishers, Dordrecht, (1999); (c) Lehn J.-M., *Angew Chem Int Ed Engl* **29** (1990) 1304; (d) Aakeröy C. B., Champness N. R. and Janiak C. *Cryst Eng Comm* **12** (2010) 22; (e) Braga D., Brammer L. and Champness N. R., *Cryst Eng Comm* 7 (2005) 1.
9. Long D.-L., *et al.*, *Angew Chem Int Ed* **42** (2003) 4180.
10. (a) Long D.-L., Kögerler P. and Cronin L., *Angew Chem Int Ed* **43** (2004) 1817; (b) Goral M., *et al.*, *Dalton Trans* (2009) 6727; (c) Baffert C., *et al.*, *Dalton Trans* (2007) 4599; (d) Baffert C., *et al.*, *Chem–Eur J* **12** (2006) 8472; (e) Yan J., *et al.*, *Inorg. Chem* **49** (2010) 1819; (f) Miras H. N., *et al.*, *Chem Commun* (2008) 4703.

11. Abbas H., *et al.*, *Chem–Eur J* **11** (2005) 1071.
12. (a) Ritchie C., *et al.*, *Chem Commun* (2007) 468; (b) Ritchie C., *et al.*, *Dalton Trans* (2009) 6483; (c) Ritchie C., *et al.*, *Dalton Trans* (2009) 1587; (d) Ritchie, C., *et al.*, *Dalton Trans* (2006) 1712.
13. (a) Müller A., *et al.*, *Angew Chem Int Ed* **42** (2003) 5039; (b) Müller A., *et al.*, *Angew Chem Int Ed* **43** (2004) 4466; (c) Müller A., *et al.*, *Angew Chem Int Ed* **44** (2005) 7757; (d) Müller A., *et al.*, *Angew Chem Int Ed* **45** (2006) 460.
14. (a) Wassermann K., Dickmann M. H. and Pope M. T. *Angew Chem Int Ed Engl* **36** (1997) 1445; (b) Sadakane M., Dickman M. H. and Pope M. T. *Angew Chem Int Ed* **39** (2000) 2914.
15. Müller A., *et al.*, *Angew Chem Int Ed Engl* **30** (1991) 1674.
16. Ohlin C. A., *et al.*, *Angew Chem Int Ed* **47** (2008) 5634.
17. Nyman M., *et al.*, *Science* **297** (2002) 996.
18. Sigmon G. E., *et al.*, *Angew Chem Int Ed* **48** (2009) 2737.
19. Chubarova E. V., *et al.*, *Angew Chem Int Ed* **47** (2008) 9542.
20. (a) Schäffer C., *et al.*, *Angew Chem Int Ed* **48** (2009) 149; (b) Tsunashima R., *et al.*, *Angew Chem Int Ed* **49** (2010) 113.
21. (a) Hagrman P. J., Hagrman D. and Zubieta J., *Angew Chem Int Ed* **38** (1999) 2638; (b) Fang X., Anderson T. M. and Hill C. L., *Angew Chem Int Ed* **44** (2005) 3540; (c) Wang X. -L., *et al.*, *Angew Chem Int Ed* **45** (2006) 7411; (d) Lan Y. Q., *et al.*, *Chem Commun* (2008) 58.
22. Gopalakrishnan J., *Chem Mater* **7** (1995) 1265.
23. (a) Sha J., *et al.*, *Cryst Growth Des* **7** (2007) 2535; (b) Lan Y.-Q., *et al.*, *Dalton Trans* (2008) 3824.
24. (a) Proust A., Thouvenot R. and Gouzerh P., *Chem Commun* (2008) 1837; (b) Landsmann S., Lizandara-Pueyo C. and Polarz S., *J Am Chem Soc* **132** (2010) 5315.
25. Long D.-L., *et al.*, *Dalton Trans* (2005) 1372.
26. Long D.-L., *et al.*, *J Am Chem Soc* **126** (2004) 13880.
27. Long D.-L., *et al.*, *Dalton Trans* (2006) 2852.
28. (a) Streb C. *et al.*, *Chem Eur J* **14** (2008) 8861; (b) McGlone T., *et al.*, *Chem–Asian J* **4** (2009) 1612.
29. Miras H. N., *et al.*, *Angew Chem Int Ed* **47** (2008) 8420.
30. Long D.-L., *et al.*, *Angew Chem Int Ed* **45** (2006) 4798.
31. (a) Long D.-L., *et al.*, *Angew Chem Int Ed* **44** (2005) 3415; (b) Fay N., *et al.*, *Inorg Chem* **46** (2007) 3502.

32. Long D.-L., *et al.*, *Angew Chem Int Ed* **47** (2008) 4384.
33. Yan J., *et al.*, *Angew Chem Int Ed* **48** (2009) 4376.
34. Miras H. N., *et al.*, *Dalton Trans* (2008) 214.
35. (a) Cheetham A. K., Férey G. and Loiseau T., *Angew Chem Int Ed* **38** (1999) 3268; (b) Cheetham A. K., Rao C. N. R. and Feller R. K., *Chem Commun* (2006) 4780.
36. Rodriguez-Albelo L. M., *et al.*, *J Am Chem Soc* **131** (2009) 16078.
37. Villanneau R., *et al.*, *Chem Commun* (1998) 1491.
38. Abbas H., *et al.*, *Cryst Growth Des* **8** (2008) 635.
39. Streb C., *et al.*, *Angew Chem Int Ed* **46** (2007) 7579.
40. Streb C., Long D.-L. and Cronin L., *Cryst Eng Comm* **8** (2006) 629.
41. Fang X., Anderson T. M. and Hill C. L., *Angew Chem Int Ed* **44** (2005) 3540.
42. Streb C., Long D.-L. and Cronin L., *Chem Commun* (2007) 471.
43. (a) Long D.-L., *et al.*, *Chem Asian J* **1** (2006) 352; (b) Pradeep C. P, *et al.*, *Chem Commun* (2007) 4254.
44. (a) Uchida S., *et al.*, *Angew Chem Int Ed* **41** (2002) 2814; (b) Uchida S. and Mizuno N., *J Am Chem Soc* **126** (2004) 1602.
45. Mitchell S. G., *et al.*, *Dalton Trans* (2008) 1415.
46. (a) Ritchie C., *et al.*, *Angew Chem Int Ed* **47** (2008) 6881; (b) Thiel J., *et al.*, *J Am Chem Soc* **131** (2009) 4180.
47. (a) Mitchell S. G., *et al.*, *Cryst Eng Comm* **11** (2009) 36; (b) Mitchell S. G., *et al.*, *Nat Chem* **2** (2010) 308.
48. (a) Khan M. I., *et al.*, *J Am Chem Soc* **114** (1992) 3341; (b) Müller, A., *et al.*, *Chem–Eur J* **4** (1998) 1388; (c) Han J. W. and Hill, C. L., *J Am Chem Soc* **129** (2007) 15094; (d) Hou Y. and Hill C. L., *J Am Chem Soc* **115** (1993) 11823; (e) Zeng H. D., Newkome G. R. and Hill C. L., *Angew Chem Int Ed* **39** (2000) 1771; (f) Song Y.-F., *et al.*, *Inorg Chem* **47** (2008) 9137.
49. (a) Song Y.-F., *et al.*, *J Am Chem Soc* **131** (2009) 1340; (b) Han Y., *et al.*, *Macromolecules* **42** (2009) 6543; (c) Favette S., *et al.*, *Chem Commun* (2003) 2664.
50. (a) Song Y.-F., Long D.-L. and Cronin L., *Angew Chem Int Ed* **46** (2007) 3900; (b) Song Y.-F., Long D.-L. and Cronin L., *Cryst Eng Comm* **12** (2010) 109.
51. Song Y.-F., *et al.*, *J Mater Chem* **17** (2007) 1903.
52. Zhang J., *et al.*, *J Am Chem Soc* **130** (2008) 14408.
53. Song Y.-F., *et al.*, *Chem–Eur J* **14** (2008) 2349.
54. Pradeep C. P., *et al.*, *Angew Chem Int Ed* **47** (2008) 4388.

55. Pradeep C. P., *et al.*, *Angew Chem Int Ed* **48** (2009) 8309.
56. Ritchie C., *et al.*, *Nature Chemistry* **1** (2009) 47.
57. Cooper G. J. T., *et al.*, *J Am Chem Soc* **133** (2011) 5947–5954.
58. Parenty A. D. C., *et al.*, *J Org Chem* **69** (2004) 5934–5946.
59. Cooper G. J. T. and Cronin L., *J Am Chem Soc* **131** (2009) 8368–8369.
60. Cooper G. J. T., *et al.*, *Angew Chem Int Ed* **50** (2011) 10373–10376.
61. Müller A., *et al.*, *Angew Chem Int Ed Engl* **34** (1995) 2122–2124.